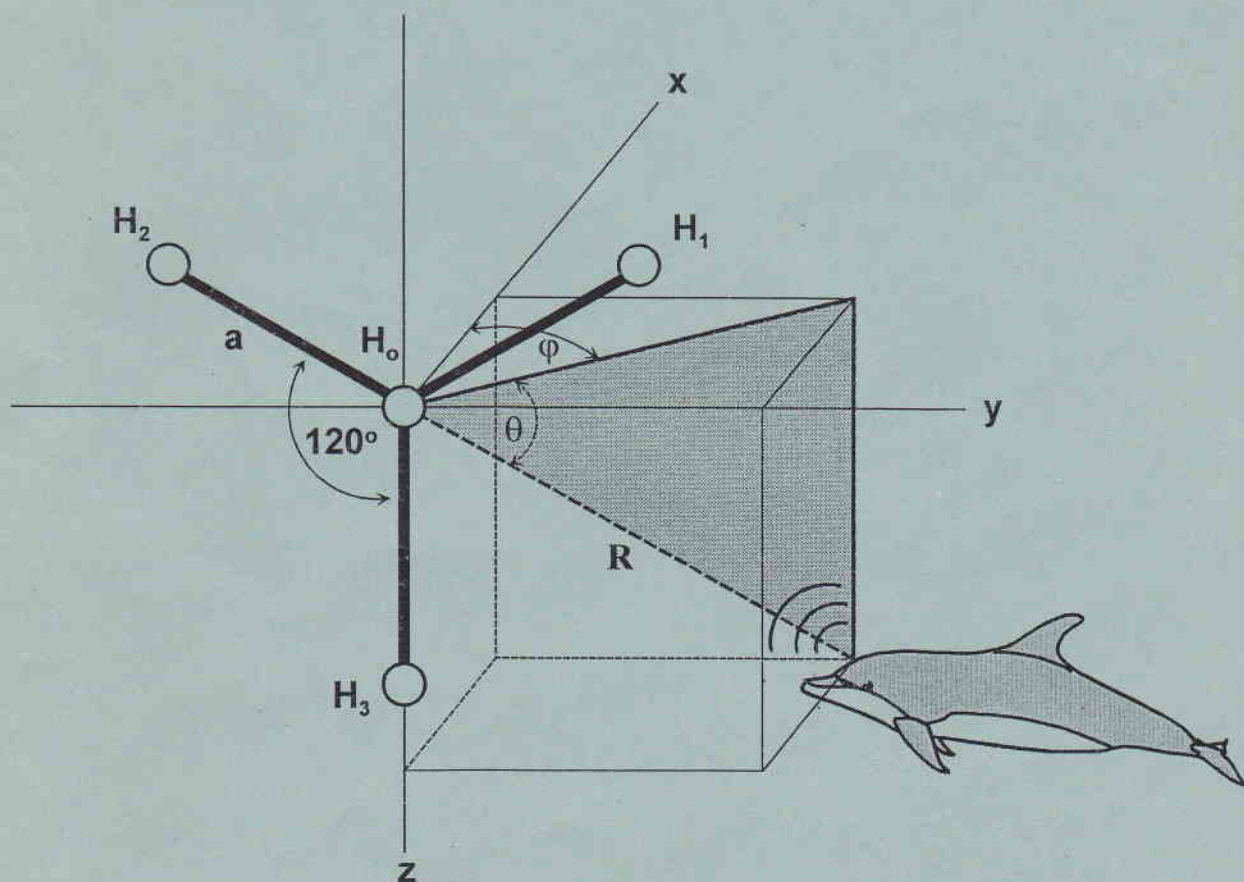


Echolocation recordings and localizations of free-ranging spinner dolphins (*Stenella longirostris*) and pantropical spotted dolphins (*Stenella attenuata*) using a four hydrophone array

Michiel Schotten



Graduate Research Report

Department of Marine Biology, University of Groningen

Supervised by Dr. Whitlow W.L. Au

Marine Mammal Research Program, University of Hawaii

September 1996 - September 1997

ABSTRACT

To get a better understanding of the use of echolocation by odontocetes in the wild, echolocation clicks of free-ranging spinner dolphins (*Stenella longirostris*) and free-ranging pantropical spotted dolphins (*Stenella attenuata*) were recorded with the use of a small, rigid, and portable symmetrical star array of four omnidirectional hydrophones. From the differences in time of click arrival at each hydrophone, locations of echolocating dolphins could be calculated to one of two points. Calibrating the array for the calculated distance showed a high accuracy of localization up to 15 m and a sufficient accuracy up to 25 m. Localizing echolocating dolphins made it possible to measure peak-to-peak source levels (SL) of the clicks, to discriminate between surface reflections and double click recordings, and to assign clicks to individual animals. Recorded clicks from both species were very much alike, with higher source levels than reported earlier for wild odontocetes (the maximum SL was 222 dB re 1 μ Pa for the spinner dolphin clicks and 220.3 dB re 1 μ Pa for the spotted dolphin clicks). Clicks were very short, broadband transient signals with high center frequencies and high intrinsic resolution capabilities, and had predominantly bimodal frequency spectra. An hypothesized subdivision of all odontocetes into two acoustic categories is further supported by these data. Furthermore, linear relationships between interclick interval and calculated distance, between center frequency and SL, and between 3-dB bandwidth and center frequency were found for both the spinner dolphin and spotted dolphin clicks.

ABSTRACT

The present study is a preliminary investigation of the effects of the use of a computer-aided instruction (CAI) program on the learning of the basic concepts of the theory of evolution. The study was conducted in a secondary school in the city of Lima, Peru. The sample consisted of 40 students in the 10th grade of secondary school. The study was divided into two groups: an experimental group and a control group. The experimental group used the CAI program, while the control group used a traditional textbook. The results of the study showed that the experimental group achieved significantly higher scores than the control group in the post-test. This suggests that the use of a CAI program can be an effective method for teaching the theory of evolution. The study also found that the experimental group showed a higher level of motivation and interest in the subject matter. These findings have important implications for the design of educational materials and the use of technology in the classroom. Further research is needed to explore the long-term effects of CAI on student learning and to identify the most effective instructional strategies for this type of content.

Echolocation recordings and localizations of free-ranging spinner dolphins (*Stenella longirostris*) and pantropical spotted dolphins (*Stenella attenuata*) using a four hydrophone array

Graduate Research Report of Michiel Schotten
September 1996 - September 1997

Department of Marine Biology, University of Groningen
P. O. Box 14
9750 AA Haren
The Netherlands

e-mail : o k̄uej qwgpB j qwo ck̄ēqo

Supervised by Dr. Whitlow W.L. Au
Marine Mammal Research Program
Hawaii Institute of Marine Biology, University of Hawaii
P. O. Box 1106
Kailua, Hawaii 96734

CONTENTS

Introduction	1
Material & Methods	5
Localizing dolphins using time of arrival differences	5
Building of the array	8
Data acquisition	10
Study site and spinner and spotted dolphin populations	10
Data analysis: localizing dolphins	10
Calibration	12
Data analysis: calculating click characteristics	13
Results	21
Analysis of single echolocation clicks	21
Double clicks	29
Characteristics of the spinner and spotted dolphin clicks	31
Assigning clicks to individual animals	33
Click trains of a spinner and a spotted dolphin	36
Relationships between click parameters	40
Discussion & Conclusions	47
Type of array and method of localizing	47
Provided solutions to problems of recording clicks at sea	48
Characteristics of the recorded clicks	50
Recommendations for further research	50

Acknowledgments	53
References	55
Appendix	57
Direct and surface reflected paths to the four hydrophones	57
Distributions of several click characteristics	62

INTRODUCTION

Since the discovery of echolocation in the bottlenose dolphin (*Tursiops truncatus*) by McBride in 1947 (McBride 1956), much research has been done (see Au 1993) on the physiology of the sonar transmission and receiving systems, the acoustic properties of the transmitted signals and their beam patterns, and on the dolphin's target detection, discrimination and recognition capabilities. Also, several signal processing models have been constructed as well. Most research has been performed on captive animals of three species of odontocetes: the bottlenose dolphin (*Tursiops truncatus*), the beluga or white whale (*Delphinapterus leucas*), and the false killer whale (*Pseudorca crassidens*). Echolocation, however, has also been demonstrated in a number of other odontocete species.

In spite of the large amount of data derived from captive animals on what the active sonar system is capable of doing, almost nothing is known about the actual use of echolocation in the wild and its ecological significance. Several functions have been proposed, the most obvious being prey and predator detection and navigation. One way to differentiate between echolocation for the purpose of either foraging or navigating is to look at click repetition rates (also referred to as interclick intervals), that are more variable during foraging than during navigation because of the movement of prey. Also, clicks used for navigation near shore are likely to be of less intensity than clicks used for foraging, since topographic features produce strong echoes (Barrett-Lennard et al. 1996). Besides catching swimming prey with the help of echolocation, Atlantic spotted dolphins (*Stenella frontalis*) and bottlenose dolphins (*T. truncatus*) have also been observed producing clicks while digging for buried prey in sandy bottoms; interclick intervals were as short as 2 ms (Herzing 1996).

Other hypothesized functions for echolocation clicks of wild odontocetes include the stunning of prey by means of high intensity clicks (Norris & Møhl 1983) and communication (Watkins 1980a; Dawson 1991). Supporting this latter possibility, Barrett-Lennard et al. (1996) found that echolocation use per individual killer whale (*Orcinus orca*) decreased with increasing group size, suggesting the sharing of information between group members. Norris et al. (1994) reported that members of dolphin schools are likely to trade the "duty" of echolocation (which is physiologically expensive) among individuals, so that only a limited number of dolphins are engaged in echolocation at any given time and information is therefore shared. The same researchers also recorded small bursts of clicks during turning maneuvers of spinner dolphin (*Stenella longirostris*) schools, which possibly serve to synchronize movements of the school.

Besides the functional question of echolocation in the wild, other questions (Au 1993) on which research needs to be focused are: what ranges are usually involved, is the use of echolocation dependent on the type of environment and time of the day (e.g. the light-dark cycle), and how often is sonar used in general? Fenton (1980) pointed out several possible constraints on the use of echolocation by bats in a natural situation, that may also apply to odontocetes. These constraints include eavesdropping by competitors

and predators, as well as alerting of prey. Indeed, Barrett-Lennard et al. (1994) found that a fish-eating population of 'resident' killer whales (*O. orca*) produced echolocation click trains of longer duration and more often than the population of mammal-eating 'transient' killer whales did, the latter being more likely to alert their prey by transmitting clicks than the former.

Compared to echolocation, listening may play a larger role in finding and catching prey than suspected previously. Wood and Evans (1980) describe how a blindfolded *Tursiops* followed and caught a live fish (a sargo, *Anisotremus davidsoni*) that was introduced in her tank up to five times in a row, without transmitting any detectable sound. According to Evans and Awbrey (1988), bottlenose dolphins in the wild also have been observed feeding "silently" in very turbid waters. Additionally, Barrett-Lennard et al. (1996) found that transient killer whales (*O. orca*) often traveled or foraged without discernibly echolocating.

Before any questions concerning the use of echolocation in the wild can be answered, it is first necessary to describe the physical characteristics of clicks that are transmitted by free-ranging odontocetes. Once these click characteristics are known, an attempt can be made to associate them with certain behaviors, such as the association between feeding behavior and certain characteristics of the signals found by Dawson (1991) for Hector's dolphin (*Cephalorhynchus hectori*).

Acoustically, it seems that odontocetes can be divided into two categories (Au pers. comm.). The first category contains all species that can produce both long-duration, frequency modulated tonal sounds as well as pulsed sounds (either echolocation clicks or burst pulse clicks). Burst pulse clicks are thought to have interclick intervals that are too short to be of use for echolocation. Clicks can extend to frequencies greater than 150 kHz, are broadband and have a duration of 50 to 100 μ s, while whistles are frequency modulated tones up to 20 kHz which can have harmonics up to around 120 kHz (Lammers pers. comm.) and lasting 0.1 to several seconds. A common representative of this category is *Tursiops*.

The second category contains all species that are known to produce only pulsed sounds. These pulsed sounds are narrow-band, with a duration of 80 to 800 μ s (Thorpe et al. 1991). Representatives of this category are members of the family *Phocoenidae* (the porpoises; Evans et al. 1988), members of the genus *Cephalorhynchus* (Dawson 1988; Dawson 1991; Thorpe et al. 1991) and the pygmy sperm whale (*Kogia simus*; Carder et al. 1995).

This subdivision into two acoustic categories might have implications concerning the different uses of clicks. Therefore, it would be worthwhile to record and analyze clicks from all free-ranging odontocete species using similar, high frequency (up to 200 kHz) broadband equipment. No such click descriptions have been found in the literature for either spinner dolphins (*S. longirostris*) or pantropical spotted dolphins (*S. attenuata*). Both species, like all species from the genus *Stenella*, are known to produce whistles (Norris et al. 1994).

When recording echolocation clicks of wild dolphins, a number of problems have to be dealt with. First, it is not known which animal produces the clicks (Watkins 1980b), making it very hard to 1) find any associations between click characteristics and behaviors, 2) ascribe certain click characteristics to individual animals, or 3) find out how many animals are clicking. Second, it is difficult to find the source level (SL) of recorded clicks, which is defined as the sound pressure level (SPL) at 1 m from the source. To determine SL, the acoustic transmission loss must be accounted for, making it necessary to know the distance from the hydrophone to the echolocating dolphin which is usually difficult to estimate with any accuracy (especially since it is not known which animal is clicking). Third, terminations of clicks are often lost in reverberation and reflections from the water surface (Watkins 1980b). Fourth, the orientation of the dolphin head relative to the hydrophone is usually unknown (Watkins & Schevill 1974; Watkins 1980b; Evans & Awbrey 1988; Dawson & Thorpe 1990). Since dolphin echolocation clicks are known to be transmitted from the melon in a narrow beam (see Au 1993), both amplitude (expressed as SPL) and frequency content of recorded clicks can be highly variable. For *Tursiops*, only clicks recorded at approximately 5° above the longitudinal axis in the vertical plane and at 0° in the horizontal plane (see Au 1993) would represent the actual clicks.

A method used in the past (Thorpe et al. 1991; Kamminga et al. 1993) to deal with this problem is to only analyze high amplitude clicks, since those clicks are most likely to be recorded from the center of the beam. However, by using this method low SL clicks recorded from the center of the beam could be missed, while high SL clicks that are off-axis could be selected. Furthermore, high SL clicks may have a higher center frequency, as shown for the false killer whale (*P. crassidens*) by Au et al. (1995), so that clicks that are analyzed by using the above method could give only a partial impression of a species' click characteristics. A better solution would be to use an underwater camera, connected to a VCR that is synchronized with the click recording device. In this way, only those clicks would be analyzed where the dolphin's head is directed towards the hydrophone, irrespective of whether they are high amplitude clicks or not.

A solution to the first and second problem (those of assigning clicks to individual animals and estimating range to calculate SL) would be finding a method to know the exact position of echolocating animals. Such a method is available from acoustics: the position of a sound source can be calculated by using an array of receivers. Since each receiver has a different distance to the sound source, the produced sounds will arrive at each receiver at different times. From the time of arrival differences, one or more positions can be calculated. Whether or not there is an ambiguity in the localization depends on the number of receivers and their mutual arrangement. The use of multiple receivers could also be a solution to the third problem (that of determining the end of actual clicks), by comparing each recorded click between different channels.

Arrays that have been used in the past to localize marine mammals by their vocalizations include a towed 45 m long line array of more than 200 hydrophones (Thomas et al. 1986), a nonrigid line array of three hydrophones spaced more than 2 km apart (Levenson 1974) and a nonrigid array of three hydrophones spaced 30 m apart (Møhl et al. 1990). By using a line array of three or more hydrophones spaced equal

distances apart, it is possible to determine the distance to the sound source, but not the direction.

However, if four hydrophones are arranged in a configuration other than a line, it is possible to determine the exact position of the sound source to one of two points. Watkins & Schevill (1974) used an array of four hydrophones spaced 30 m apart at the vertices of a tetrahedron to localize spinner dolphins (*S. longirostris*). Although dolphins inside the array could be localized with an accuracy of within 1 m, disadvantages are that this type of array is nonrigid, that it needs buoys and cables, and that it requires constant calibration using an acoustic pinger. Furthermore, due to the large size of the array, directional echolocation clicks (recorded up to 16 kHz) were seldom heard on all four hydrophones, and thus could not be localized. Instead, localizations were done using burst pulse sounds, that according to the authors did not appear to be particularly directional.

In order to localize dolphins by detecting their echolocation clicks, an array that is small, rigid and portable would be needed. This paper describes how a four hydrophone symmetrical star array (adopted from Aubauer 1995) with a flat frequency response up to 160 kHz was used to localize free-ranging spinner dolphins (*S. longirostris*), free-ranging pantropical spotted dolphins (*S. attenuata*), and captive bottlenose dolphins (*T. truncatus*). Furthermore, a detailed analysis of the recorded echolocation clicks is presented.

MATERIALS & METHODS

Localizing dolphins using time of arrival differences

When the plane of a four hydrophone symmetrical star array is taken as the y-z plane of a Cartesian coordinate system with the center hydrophone (H_0) as the origin (Fig. 1), the coordinates of the echolocating dolphin can be expressed as the distance from H_0 to the dolphin (range R), the horizontal angle φ and the vertical angle θ , as follows (see Fig. 1):

$$x = R \cdot \cos\varphi \cdot \cos\theta$$

$$y = R \cdot \sin\varphi \cdot \cos\theta$$

$$z = R \cdot \sin\theta$$

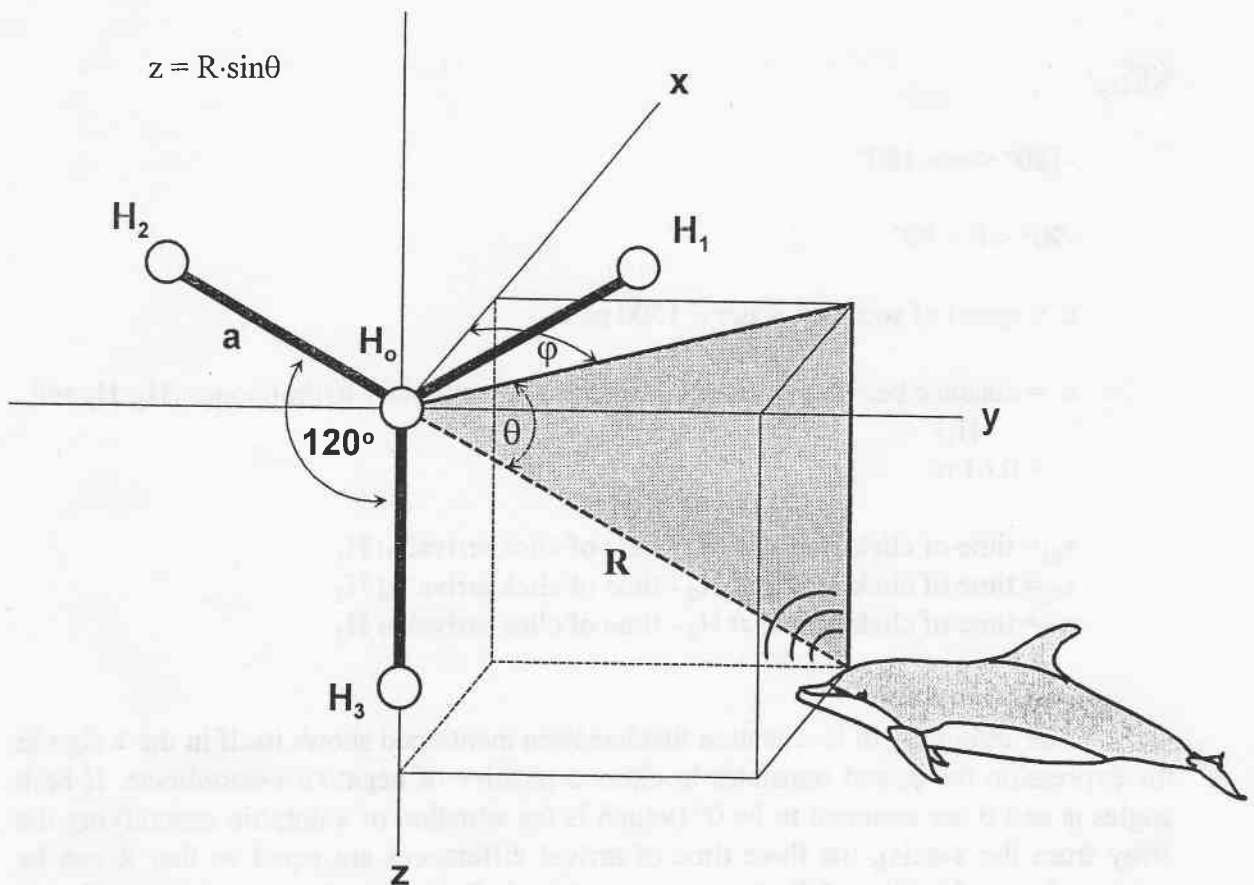


Fig. 1. In a 3D Cartesian coordinate system, the position of a dolphin echolocating on a four hydrophone symmetrical star array can be expressed as a range R to the center hydrophone H_0 , a horizontal angle φ , and a vertical angle θ . Distance a between H_0 and each of the outer hydrophones H_1 , H_2 , and H_3 is 0.61 m. In the above coordinate system, the echolocating dolphin has a positive x -coordinate, but negative y and z coordinates. Therefore, both φ and θ have negative values as well.

Therefore, to localize the dolphin it is sufficient to know R , φ and θ . If the coordinate system is defined as in Fig. 1, these values can be derived using the above expressions and Pythagoras' theorem to be (Aubauer 1995):

$$R = \frac{c^2 (\tau_{01}^2 + \tau_{02}^2 + \tau_{03}^2) - 3a^2}{2c (\tau_{01} + \tau_{02} + \tau_{03})}$$

$$\varphi = 90^\circ \pm \arccos \left(\frac{2cR (\tau_{02} - \tau_{01}) + c^2 (\tau_{01}^2 - \tau_{02}^2)}{2 \sqrt{3a^2 R^2 - 0.75 (2Rc\tau_{03} - c^2 \tau_{03}^2 + a^2)^2}} \right)$$

$$\theta = -\arcsin \left(\frac{2Rc\tau_{03} - c^2 \tau_{03}^2 + a^2}{2aR} \right)$$

where:

$$-180^\circ < \varphi < 180^\circ$$

$$-90^\circ < \theta < 90^\circ$$

c = speed of sound in water ≈ 1500 m/s

a = distance between center hydrophone (H_0) and outer hydrophones (H_1 , H_2 and H_3)
= 0.61 m

τ_{01} = time of click arrival at H_0 - time of click arrival at H_1

τ_{02} = time of click arrival at H_0 - time of click arrival at H_2

τ_{03} = time of click arrival at H_0 - time of click arrival at H_3

The ambiguity in localization that has been mentioned shows itself in the \pm sign in the expression for φ , and translates in either a positive or negative x-coordinate. If both angles φ and θ are assumed to be 0° (which is the situation of a dolphin ensonifying the array from the x-axis), the three time of arrival differences are equal so that R can be expressed as a function of $\Sigma\tau$ ($= \tau_{01} + \tau_{02} + \tau_{03}$). From Fig. 2, it can be seen that R becomes unrealistically large at very small $\Sigma\tau$. For this reason, only ranges up to an arbitrary value of 30 m ($\Sigma\tau \approx -11 \mu\text{s}$) are said to be reliable. Thus, calculated ranges higher than 30 m are rejected beforehand.

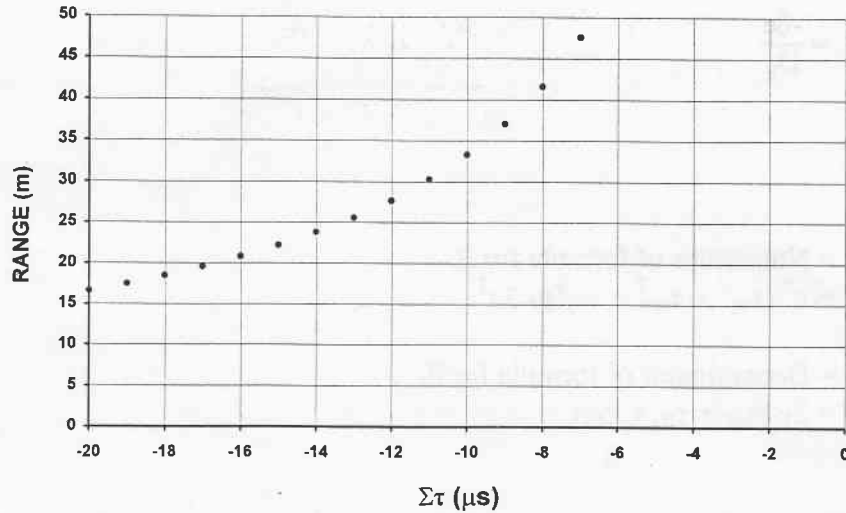


Fig. 2. Increasing range with increasing sum of time of arrival differences, calculated for $\varphi = 0^\circ$ and $\theta = 0^\circ$. For $R > 30$ m, R increases > 6 m for each $2 \mu\text{s}$ increase of $\Sigma\tau$.

This could also be concluded from looking at the theoretical error in range estimation, which can be expressed as (Aubauer 1995):

$$\Delta R = \left| \frac{\partial R}{\partial \tau_{01}} \right| \Delta \tau_{01} + \left| \frac{\partial R}{\partial \tau_{02}} \right| \Delta \tau_{02} + \left| \frac{\partial R}{\partial \tau_{03}} \right| \Delta \tau_{03} + \left| \frac{\partial R}{\partial a} \right| \Delta a$$

where:

$\Delta \tau_{01}, \Delta \tau_{02}, \Delta \tau_{03}$ = assumed deviations in time of arrival differences
 = $3 \mu\text{s}$ (see next section)

Δa = assumed deviation in a
 = 1 cm

$$\frac{\partial R}{\partial \tau_{01}} = \frac{2\tau_{01}c^2D_R - N_R2c}{D_R^2}$$

$$\frac{\partial R}{\partial \tau_{02}} = \frac{2\tau_{02}c^2D_R - N_R2c}{D_R^2}$$

$$\frac{\partial R}{\partial \tau_{03}} = \frac{2\tau_{03}c^2D_R - N_R2c}{D_R^2}$$

$$\frac{\partial R}{\partial a} = \frac{-6a}{D_R}$$

and:

$$N_R = \text{Numerator of formula for } R \\ = c^2 (\tau_{01}^2 + \tau_{02}^2 + \tau_{03}^2) - 3a^2$$

$$D_R = \text{Denominator of formula for } R \\ = 2c (\tau_{01} + \tau_{02} + \tau_{03})$$

In Fig. 3, ΔR is plotted against R for several assumed deviations in time of arrival differences $\Delta\tau$ (either $\Delta\tau_{01}$, $\Delta\tau_{02}$ or $\Delta\tau_{03}$). It can be seen that ΔR increases with increasing R and increasing $\Delta\tau$.

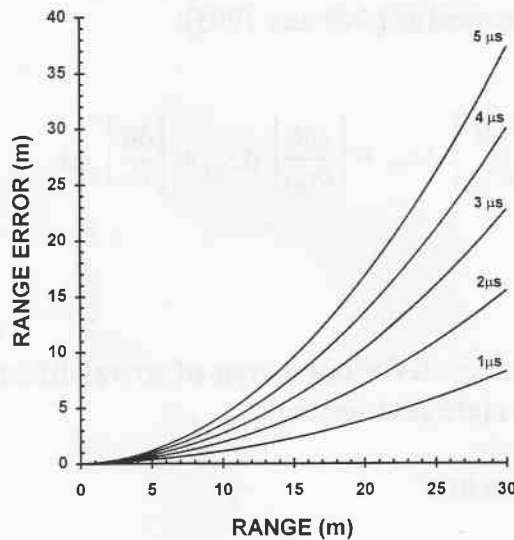


Fig. 3. Theoretical ΔR as a function of R, for an assumed $\Delta\tau$ ($\Delta\tau_{01}$, $\Delta\tau_{02}$ and $\Delta\tau_{03}$) of either 1, 2, 3, 4 or 5 μs . Δa is assumed to be 1 cm.

Building of the array

A four hydrophone symmetrical star array (Fig. 4) was built using a 5.08 cm thick rectangular block of delrin mount, that was connected via 1.27 cm diameter pvc-pipes to four omnidirectional ITC 1094 A hydrophones with a flat frequency response up to 160 kHz. Pvc-pipe was chosen because of its small acoustic reflectivity (Au pers. comm.). The three outer hydrophones were separated at angles of 120° and spaced 61.0 cm from the center hydrophone, H_0 . The plane of the hydrophones was located 8.5 cm parallel from the block of delrin mount and 9.1 cm from the outsticking pvc-pipes. It was assured

several times that all four hydrophones were still in the exact same plane, since a deviation of only 3 mm from the plane would cause a deviation of $2 \mu\text{s}$ ($= 3 \text{ mm} / 1500 \text{ ms}^{-1}$) in a time of arrival difference. Two of the four hydrophones had deviations of up to 5 mm out of the plane, corresponding to a $\Delta\tau$ of around $3 \mu\text{s}$ which was used to calculate ΔR in the later data analysis (so that, theoretically, $\Delta R = 16.0 \text{ m}$ at $R = 25 \text{ m}$, see Fig. 2). However, these deviations were apparently canceled out if the three time of arrival differences were added, since the results of the range calibration of the array showed a ΔR of only 3.4 m at $R = 25 \text{ m}$ (see the regarding section). During all echolocation recordings the four hydrophones stayed approximately in the same place with deviations of up to 1 mm.

The hydrophone cables were connected to a rechargeable battery-driven, multi-channel pre-amplifier/linedriver with a 18 dB gain and a flat frequency response up to 200 kHz, housed in a water-tight box that was attached to the delrin mount block. The pre-amplifier was connected via cables feeding back to the boat to a rechargeable battery-driven, multi-channel amplifier with an adjustable gain for each channel and a flat frequency response up to 200 kHz. A 5.08 cm diameter metal pipe was connected to the block to stick the array in the water. A small video camera in a water-tight transparent container was attached to the metal pipe, approximately 10 cm above H_0 . It was connected to a VCR on the boat that was synchronized with the data acquisition system. The array could be taken apart and put back together again with a screwdriver.

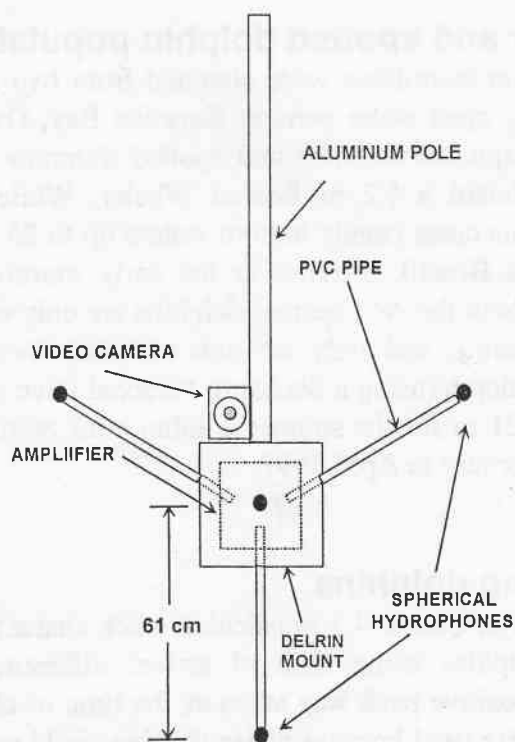


Fig. 4. The hydrophone array that was used for data acquisition.

Data acquisition

Instead of storing the incoming acoustic signals on an analog recording device, immediate analog-to-digital conversion was accomplished by using two GAGE 1210, 12 bit dual simultaneous sampling data acquisition boards, that were connected to internal slots of a transportable "lunch box" type computer (a Portable Expandable Platform 486 DX-33). Power was supplied by a 12 V rechargeable battery box connected to a 150 W DC/AC inverter (Statpower). Analog-to-digital conversion was performed at a sample rate of 500 kHz, so that every 2 μ s a digitized point was added.

The data acquisition system was driven by a program written in Qbasic 4.5 and operated with a pre-trigger capability, meaning that incoming signals were continuously digitized and fed into temporal memory, until the amplitude of a signal would exceed a pre-set value and thus trigger the transfer of a number of digitized points before and after the onset of the signal to the board's normal memory. The data collection process for all four channels was triggered by the input of the center hydrophone, H_0 . Both the number of pre-trigger points and post-trigger points were set at 200, so that 800 μ s were stored per channel every time an echolocation click was detected. Up to 80 consecutive clicks could be stored each time into one file, together with the time (to synchronize with video recordings) and interclick intervals (ICI) in ms for each click.

Study site and spinner and spotted dolphin populations

Preliminary echolocation recordings were obtained from two adult male captive *Tursiops* swimming in floating open water pens in Kaneohe Bay, Oahu, Hawaii. Next, recordings from free-ranging spinner dolphins and spotted dolphins were made at the Waianae coast of Oahu on board a 5.2 m Boston Whaler. While spinner dolphins frequently visit two areas of this coast (sandy bottom waters up to 25 m deep in front of Kahe Beach Park and Makua Beach), arriving in the early morning and sometimes staying at the same site throughout the day, spotted dolphins are only encountered on rare occasions (Lammers pers. comm.), and only on one occasion their clicks could be recorded. The measured water depth (using a Scubapro Personal Dive Sonar 2) was 40 m, while depth varied from 6 to 21 m for the spinner dolphin click recordings which were obtained on four days from February to April 1997.

Data analysis: localizing dolphins

A program was written in Qbasic 4.5 to calculate click characteristics, as well as positions of echolocating dolphins using time of arrival differences. The point of appearance of the maximum positive peak was taken as the time of click arrival at each channel. No negative peaks were used because phase shifting could cause the maximum absolute amplitude of the click to appear at a different position within the click on each channel. Using only positive peaks made it easier to assure that the same excursion was taken as time of click arrival on all four channels. This was important because the calibration showed that the use of a different excursion of the signals between channels could cause large errors in range estimations. If one channel had its maximum peak at an

excursion that was different compared to the other channels, the correct excursion could be selected manually on that channel by means of a cursor option. This option consisted of two cursors that reset all digitized points to zero, either before or after the point where the cursor was positioned.

To obtain the most accurate estimation of the actual peak appearance within the excursion (since digitized points were sampled only every $2 \mu\text{s}$), a 3-point parabolic curve fit was calculated through the point with the maximum amplitude (point 2) and the points preceding and following that point (points 1 and 3). If $x_2 = 0$, $x_1 = -1$ and $x_3 = 1$, the x-value x_p of the peak of the parabola can be expressed as:

$$x_p = \frac{y_1 - y_3}{2(y_1 + y_3 - 2y_2)}$$

where:

$$y_1, y_2, y_3 = \text{amplitudes of points 1, 2, 3 } (y_2 > y_1 \wedge y_2 > y_3)$$

The time of the estimated maximum peak can now be expressed as:

$$t_p = (x_2' + x_p) \cdot 2 \mu\text{s}$$

where:

$$x_2' = n^{\text{th}} \text{ digitized point representing point 2}$$

The time of arrival differences are:

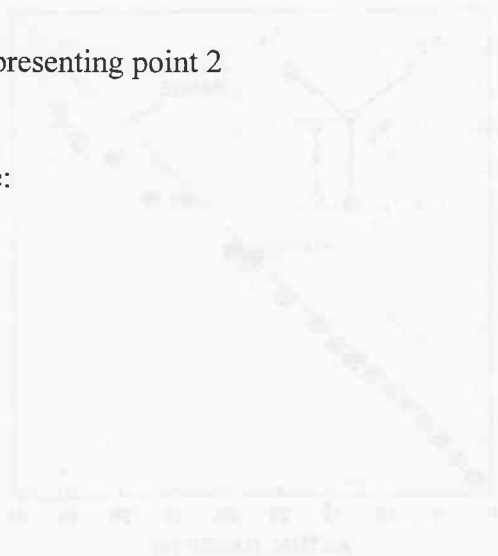
$$\tau_{01} = t_{p0} - t_{p1}$$

$$\tau_{02} = t_{p0} - t_{p2}$$

$$\tau_{03} = t_{p0} - t_{p3}$$

where:

$$t_{p0}, t_{p1}, t_{p2}, t_{p3} = t_p \text{ on channel 0, 1, 2, 3}$$



The use of the 3-point parabolic curve fit proved to give the least variation in calculated positions between clicks, and also gave the best results in the performed calibration. From τ_{01} , τ_{02} , and τ_{03} , values were calculated for R , θ , ϕ_1 , ϕ_2 , and ΔR . Depth of the dolphin could be estimated to be depth D of H_0 (assumed to be 1.5 m) + $R \cdot \sin(-\theta)$. These parameters, including τ_{01} , τ_{02} , τ_{03} , click number, time, and interclick interval (ICI), were written to a separate file.

Calibration

To measure the accuracy of range calculations, a calibration was performed by transmitting trains of a digitized *Tursiops* click underwater and recording them with the hydrophone array at different distances from the transmitter. Source levels of transmitted clicks were 208 ± 2 dB re $1 \mu\text{Pa}$ and interclick intervals were 500 ± 10 ms. The array was held so that H_0 was at the same depth as the transmitter (thus, $\theta \approx 0^\circ$) and the plane of the array was parallel to the plane of the transmitter (thus, $\phi \approx 0^\circ$). The mean ranges that were calculated by the program (n varied from 9 to 17 clicks for each range) were plotted against the actual ranges (Fig. 5). It shows that range is increasingly underestimated as range increases, but still within acceptable limits. Standard deviations also increase with range but remain very small (< 0.7).

The array was only calibrated for calculations of R , not for calculations of ϕ or θ (although both ϕ and θ were calculated by the program to be $\pm 0^\circ$). According to Watkins and Schevill (1974), estimations of directions inherently are more accurate than estimations of range in passive acoustic localization. Besides, accuracy in estimation was more important for R than for ϕ and θ , since R was used to calculate click source levels.

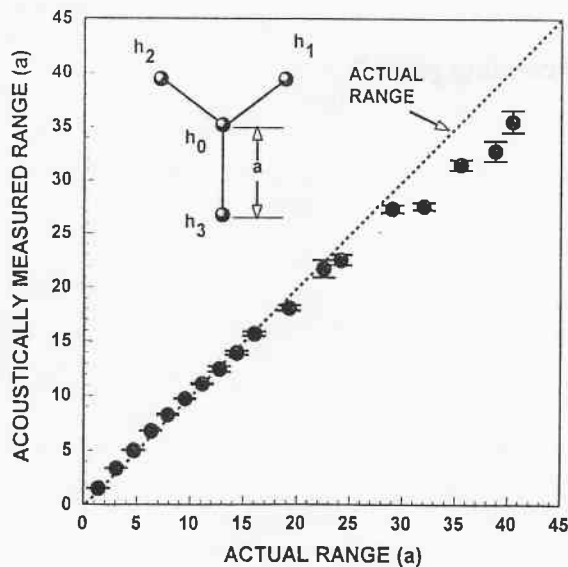


Fig. 5. Array calibration for calculations of R , expressed in a ($a = 0.61$ m).

Data analysis: calculating click characteristics

A further analysis of each recorded click was performed on the channel with the highest absolute amplitude. This channel was assumed to have recorded the click from most closely to the center of the echolocation transmission beam, thus representing the 'real' click most closely. To select the recorded click without its reflection from the water surface and without low-frequency background noise, the same cursor option as described earlier was used.

For each click selection, a subjective decision had to be made on where the click ended and where the surface reflection began, since clicks and surface reflections interfered sometimes. This decision was mainly based on the fact that surface reflections mirror the click in amplitude (that is, positive peaks in the click appear as negative peaks in surface reflections, and vice versa), due to the large impedance difference between water and air. Another tool was to look at the time between the click and its surface reflection. This time Δt is expected to be different for each channel, due to different distances that the click and its surface reflection have to travel to each hydrophone. The largest Δt can be expected for the deepest hydrophone, which is H_3 .

If a flat water surface is assumed, with the pole of the array (the z-axis in Fig. 1) exactly perpendicular to it, Δt can also be expressed mathematically as:

$$\Delta t_i = (R_i - SR_i)/c$$

where:

$i = 0, 1, 2,$ or $3,$ for hydrophones $H_0, H_1, H_2,$ and $H_3,$ respectively

$c \approx 1500$ m/s

R_i = direct path from the dolphin to hydrophone $i.$

SR_i = surface reflected path from the dolphin to hydrophone $i.$

The four ranges from the dolphin to the four hydrophones can be expressed as (see Appendix):

$$R_0 = R$$

$$R_1 = \sqrt{R^2 + a^2 + a \cdot R \cdot \sqrt{3} \cdot \sin\phi \cdot \cos\theta - a \cdot R \cdot \sin\theta}$$

$$R_2 = \sqrt{R^2 + a^2 - a \cdot R \cdot \sqrt{3} \cdot \sin\phi \cdot \cos\theta - a \cdot R \cdot \sin\theta}$$

$$R_3 = \sqrt{R^2 + a^2 + 2 \cdot a \cdot R \cdot \sin\theta}$$

The four surface reflected paths are:

$$SR_0 = \sqrt{R^2 + 4 \cdot D^2 - 4 \cdot R \cdot D \cdot \sin\theta}$$

$$SR_1 = \sqrt{R^2 + 4 \cdot D^2 - 3 \cdot a \cdot D + 1.5 \cdot a^2 + a \cdot R \cdot \sqrt{3} \cdot \sin\phi \cdot \cos\theta - 2 \cdot R \cdot D \cdot \sin\theta}$$

$$SR_2 = \sqrt{R^2 + 4 \cdot D^2 - 3 \cdot a \cdot D + 1.5 \cdot a^2 - a \cdot R \cdot \sqrt{3} \cdot \sin\phi \cdot \cos\theta - 2 \cdot R \cdot D \cdot \sin\theta}$$

$$SR_3 = \sqrt{R^2 + 4 \cdot D^2 + 4 \cdot a \cdot D + a^2 - 2R \cdot (2D + a) \cdot \sin\theta}$$

where D is depth of H_0 and is assumed to be between 0.5 and 2 m. Due to wave action, varying values for D , and angles other than 90° between the array pole and water surface, the equations for SR_i (and therefore for Δt_i) will often be inaccurate. However, they can give a rough indication and can be used in deciding what is surface reflection and what not. Generally, the farther away the dolphin is from the array, and the closer it is to the water surface, the shorter Δt will be.

Once the actual click was selected by using the cursor marks, the following plots were calculated and drawn on the screen:

1. The signal in the time domain, $s(t)$. This is the normalized amplitude plotted as a function of time:

$$s(t) = \frac{p(t)}{p_{\max}}$$

where:

$p(t)$ = acoustic pressure as a function of time, in μPa

p_{\max} = absolute maximum acoustic pressure, in μPa (that is, the biggest peak in amplitude, either positive or negative)

2. The envelope of the signal, which emphasizes all the main oscillations of $s(t)$ and ignores the higher frequency oscillations. The envelope connects all the positive peaks of $s(t)$ with a single line, and can be expressed as $\sqrt{s^2(t) + \hat{s}^2(t)}$, where $\hat{s}(t)$ is the so-called imaginary part (containing negative frequencies) of the analytic signal $s_a(t)$, and $s_a(t) = s(t) + j\hat{s}(t)$. The imaginary part of the analytic signal, $\hat{s}(t)$, is the Hilbert transform of the real part, $s(t)$.

3. The spectrum, or the signal in the frequency domain, $S(f)$. This is the normalized amplitude plotted as a function of frequency. $S(f)$ can be calculated by taking the Fast Fourier Transform (FFT) of $s(t)$.

4. Furthermore, there was an option for plotting the envelope of the so-called wideband ambiguity function, $\chi(\eta, \tau)$, or $\chi(v, r)$, on the screen. The ambiguity function of an echolocation click indicates the theoretical target resolution that the click provides, for different velocities of the target relative to the echolocating dolphin. Thus, by looking for a change in target resolution at different velocities, it can also be seen how well a single echolocation click provides information on target velocity. For the *Tursiops* click, no such information is provided (Au 1993).

The wideband ambiguity function can be expressed as:

$$\chi(\eta, \tau) = \frac{1}{\sqrt{\eta}} \mathfrak{F}^{-1} \left[S(f) \cdot S\left(\frac{f}{\eta}\right) \right]$$

where:

η = Doppler scale factor

$$= \frac{1 + \frac{v}{c}}{1 - \frac{v}{c}}$$

v = velocity of the target relative to the echolocating dolphin

$c \approx 1500$ m/s

τ = time delay between the transmitted click and its returning echo

$$\mathfrak{F}^{-1} \left[S(f) \cdot S\left(\frac{f}{\eta}\right) \right] = \text{inverse Fourier transform or inverse FFT of } \left[S(f) \cdot S\left(\frac{f}{\eta}\right) \right]$$

$S(f)$ = frequency domain of the signal

The envelope of $\chi(\eta, \tau)$ (called the ambiguity density) was plotted as a function of the relative target velocity v and the range r , rather than η and τ (with $v = c \cdot \left(\frac{\eta - 1}{\eta + 1}\right)$ and $r = \frac{1}{2} \cdot c \cdot \tau$).

Besides drawing the above plots, the program also calculated the following click characteristics:

1. SPL = peak-to-peak sound pressure level, in dB re 1 μ Pa
 $= 20 \log(p_{pkpk})$
 $= |H_S| - G_A + 20 \log(V_{pkpk})$

where:

- p_{pkpk} = peak-to-peak acoustic pressure, in μPa
- $|H_S|$ = hydrophone sensitivity = 215 dB re 1 V / μPa
- G_A = gain of amplifiers = 36 or 42 dB
- V_{pkpk} = peak-to-peak voltage, A/D adjusted, in V
- = voltage of highest positive peak + |voltage of highest negative peak|
- = constant $\cdot p_{pkpk}$

The constant depends on H_S , G_A and on A/D conversion parameters. Since the maximum voltage that the boards were programmed to digitize was ± 5 V, the SPL could get saturated at either 193, 197 or 199 dB re 1 μPa , dependent on the gain that the amplifier was adjusted to.

- 2. SL = peak-to-peak source level, in dB re 1 μPa
= SPL + 20 logR + αR

where:

$$\alpha = \text{acoustic absorption coefficient, in dB / m}$$

For $R < 30$ m, α does not significantly contribute to transmission loss and can therefore be ignored (Au 1993). The 20 logR term is referred to as the spherical spreading loss.

- 3. SL_{min} = theoretical minimum peak-to-peak source level
= SPL + 20 log(R - ΔR)

- 4. SL_{max} = theoretical maximum peak-to-peak source level
= SPL + 20 log(R + ΔR)

- 5. SE = source energy flux density, in dB re 1 $\mu\text{Pa}^2\text{s}$
= $10 \log \int_0^T p^2(t) dt + 20 \log R$

- 6. E_N = normalized energy, in dB
= energy in acoustic waveform itself, independent of amplitude
= $10 \log \int_0^T s^2(t) dt$

7. f_p = peak frequency, in kHz
 = frequency at maximum amplitude

8. f_0 = center frequency, in kHz
 = frequency that divides the energy of the spectrum into two equal parts

$$= \frac{\int_{-\infty}^{\infty} f \cdot |S(f)|^2 df}{\int_{-\infty}^{\infty} |S(f)|^2 df}$$

9. BW = 3-dB bandwidth, in kHz
 = $f_2 - f_1$

where:

$$f_1 < f_p$$

$$f_2 > f_p$$

f_1, f_2 = frequencies at an amplitude that is 3 dB re 1 Pa less than the maximum amplitude

10. β = rms (root mean square) bandwidth, in kHz

$$= \sqrt{\frac{\int_{-\infty}^{\infty} (f-f_0)^2 \cdot |S(f)|^2 df}{\int_{-\infty}^{\infty} |S(f)|^2 df}}$$

11. τ = signal duration, in μ s
 = $t_2 - t_1$

where t_1 is the time where the signal energy reaches a threshold value of 0.4% of the maximum energy and t_2 is the time where the signal energy is within 0.01% of the maximum energy; the most reliable signal durations with respect to visual comparison were obtained for these arbitrary values of 0.4% and 0.01%

12. τ_d = rms signal duration, in μs

$$= \sqrt{\frac{\int_{-\infty}^{\infty} (t-t_0)^2 \cdot |s(t)|^2 dt}{\int_{-\infty}^{\infty} |s(t)|^2 dt}}$$

13. t_0 = centroid of the time domain signal, in μs

= time after the onset of the signal that divides the energy of the time wave into two equal parts

$$= \frac{\int_{-\infty}^{\infty} t \cdot |s(t)|^2 dt}{\int_{-\infty}^{\infty} |s(t)|^2 dt}$$

14. $\tau_d \beta$ = time bandwidth product

where:

τ_d expressed in s, β expressed in Hz

$$\tau_d \beta \geq \frac{1}{4\pi} \quad (\text{sonar uncertainty principle})$$

Gabor (1947) has demonstrated that a sinusoidal pulse with a constant frequency and a Gaussian envelope is the only function that has a time bandwidth product which is equal to the lower limit of $\frac{1}{4\pi}$ (≈ 0.08). He called this the elementary signal. Thus, the $\tau_d \beta$ value of an echolocation click indicates how close the click approximates this ideal, elementary signal.

15. $\Delta\tau$ = Woodward time resolution constant, in μs
 = minimum time difference in echo arrival that is needed to recognize the echoes of two point targets as two separate echoes instead of one echo; this is a theoretical parameter that can be predicted from the spectrum of the click

$$\Delta\tau = \frac{\int_{-\infty}^{\infty} |S(f)|^4 df}{[\int_{-\infty}^{\infty} |S(f)|^2 df]^2}$$

16. Δr = range resolution, in cm
 = minimum distance between two point targets that is needed to recognize them as two separate points
 = maximum target resolution that each click can theoretically attain
 $= \frac{1}{2} \cdot c \cdot \Delta\tau$

17. $\frac{\text{Amb}(300)}{\text{Amb}(0)}$ = ambiguity density at $v = 300$ m/s and $r = 0$ m, divided by the ambiguity density at $v = 0$ m/s and $r = 0$ m.
 = an artificial parameter which can be used to compare Doppler sensitivity of a single click with that of other clicks. Although clicks with a $\frac{\text{Amb}(300)}{\text{Amb}(0)}$ close to 0 are more Doppler sensitive than clicks with a $\frac{\text{Amb}(300)}{\text{Amb}(0)}$ close to 1, these former clicks may still be very Doppler insensitive for velocities up to 20 m/s so that target velocities cannot be resolved to any useful degree from a single echo. Therefore, this parameter is only to be used for reasons of comparison.

For each click, all 17 click characteristics were written to the same file that contained the position parameters of echolocating dolphins. Next, the parameters were imported into a spreadsheet program for a more detailed analysis, such as calculating means and standard deviations and looking into any relationships between parameters.

RESULTS

Except for the preliminary recordings from captive *Tursiops*, no usable video data were obtained. The video recordings from *Tursiops* show a dolphin that is approaching the array from ± 5 m to 1 m and a stationary dolphin at ± 4 m. Both of them have their heads pointed at the array. The recorded movements agree very well with the calculated positions for each click. One reason why no other video data were obtained is because free-ranging dolphins never ensonified the array directly from the front (with $\theta = 0^\circ$ and $\varphi = 0^\circ$) and therefore were outside the visual field of the camera. Another reason is that the video equipment failed during later recordings. Therefore, it was not possible to distinguish between clicks that were off-axis (and thus not representing the actual clicks) and clicks from the center of the echolocation beam. To, nevertheless, try to use only clicks from the center of the beam, each recorded click was analyzed from the channel with the highest sound pressure level. Additionally, in situations where the highest SPL was recorded by the middle hydrophone H_0 and consequently lower amplitudes by the outer hydrophones, it could be argued that the dolphin had its echolocation beam directed at the array. Therefore, a subselection of clicks with the highest SPL at H_0 was made (referred to as H_0 -clicks), and the analysis of these subselected clicks was compared with the analysis of all clicks.

Another problem that was experienced, besides the failing video equipment, was that one or more channels (from H_1 , H_2 and H_3) sometimes failed to record due to a faulty connection. Since omitting one of the channels from the calibration data and using a formula for a three hydrophone array showed that no reliable values for R could be calculated (and that different values for R were obtained if either the channel from H_1 , H_2 or H_3 was omitted), no values for R , θ , φ_1 , φ_2 , ΔR , depth, SL , SL_{\min} , SL_{\max} and SE were obtained from clicks that had one or more channels missing. The remaining click characteristics of those clicks were used, however, in further data analysis.

A total of 851 spinner dolphin clicks and 340 spotted dolphin clicks were recorded and analyzed. Of these clicks, only 131 spinner dolphin clicks and 196 spotted dolphin clicks were recorded on all four channels. Assuming depth D of H_0 to be 1.5 m, the mean depths (\pm SD) of the localized spinner dolphin and spotted dolphin clicks were 2.8 ± 2.3 m and 1.1 ± 0.8 m, respectively. The recorded *Tursiops* clicks are not further presented here because the click characteristics of captive *Tursiops* are already well-known (see Au 1993).

Analysis of single echolocation clicks

Fig. 6 shows a typical spinner dolphin click as it was received on the four channels, with the upper channel indicating H_0 , the second channel H_1 , the third channel H_2 , and the fourth channel H_3 . The numbers at each channel indicate the time in μs from the first digitized point stored (at the left side of Fig. 6) to the maximum positive peak of the click. Thus, τ_{01} , τ_{02} , and τ_{03} can be estimated by subtracting the numbers at the second, third, and fourth channel, respectively, from the number at the first channel (the actual

time of arrival differences deviate a bit because of the use of the 3-point parabolic curve fit). The peak-to-peak sound pressure level of the click at each channel is indicated in the upper right corner of Fig. 6. The highest SPL was received at the first channel so that the recorded click can be considered as an H_0 -click, as defined before. Therefore, the first channel was most likely to have recorded the click from the beam axis, and a further click analysis was performed on this channel with the two cursor marks indicating the selected digitized points.

The part after the second cursor mark is considered to be surface reflection, based on the mirrored amplitudes of the reflection relative to the click (positive peaks become negative peaks and vice versa). It is also consistent with the time delay between the click and its surface reflection, Δt , at each channel. This time is higher for the fourth channel of the deepest hydrophone H_3 than for the first channel of H_0 , while the second and third channel, of the two shallowest hydrophones, show a lot of interference of the click with its surface reflection. By measuring the time delays Δt_0 , Δt_1 , Δt_2 , and Δt_3 from Fig. 6 and filling these in with R , θ , and ϕ in the equations mentioned in the Material and Methods, the depth D of H_0 is calculated to be 0.8 m, which seems to be a reasonable estimation.

Fig. 7 shows the results of the click analysis on the first channel. This typical spinner dolphin click had a sharp rise time and two main excursions followed by some minor excursions in the time domain, and was 36 μ s long (Fig. 7A). The envelope (Fig. 7B) shows one major and one minor oscillation, while the spectrum (Fig. 7C) was broadband and had most of its energy between 40 kHz and 120 kHz with detectable energy up to the upper limit of recording of 200 kHz. The peak-to-peak source level had a high value of 209.9 dB re 1 μ Pa, thereby classifying this click among the 30% loudest of all recorded spinner dolphin clicks that could be localized.

Fig. 8 shows another spinner dolphin click with an even higher source level of 213.5 dB, recorded from about 13 m, and also being an H_0 -click (and therefore analyzed on the first channel). The waveform (Fig. 8A) and envelope (Fig. 8B) of the click were quite similar to the click of Fig. 7. The spectrum, however, was bimodal instead of unimodal, with the low frequency peak having an almost equal but somewhat higher amplitude than the high frequency peak (Fig. 8C). The next click from the same click train was also an H_0 -click, but had a higher source level of 214.0 dB. The waveform, envelope, and spectrum look almost similar to those of Fig. 8, but this time the high frequency peak had the highest amplitude (Fig. 9).

The click with the highest source level (218.6 dB) of all recorded spinner dolphin clicks (apart from a number of clicks that had even higher source levels but were saturated on all four channels) is shown in Fig. 10. It was recorded from about 13 m and had its highest SPL at the second channel, on which it was analyzed. Generally, the loudest clicks in the recordings seemed to be more irregular in shape (sometimes having several peaks in the spectrum) and more variable than clicks that were a few dB less in amplitude.

signal # 68 intclick = 48 ms 11:02:33 SPL1 = 190.1 dB
 SPL = 190.1 dB / SL = 209.9 dB (206.5 ; 212.4) SPL2 = 188.0 dB
 range = 9.81 m (6.63 ; 12.98) SPL3 = 188.8 dB
 The = 2.9° / Depth = 1.0 m / Phi = -34.8° v -145.2° SPL4 = 187.9 dB
 Tau01 + Tau02 + Tau03 = -32 μ s

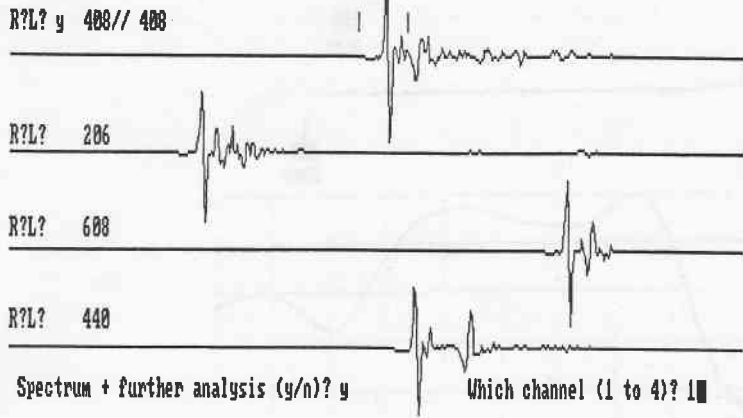


Fig. 6. A single spinner dolphin click as it was received on the four channels.

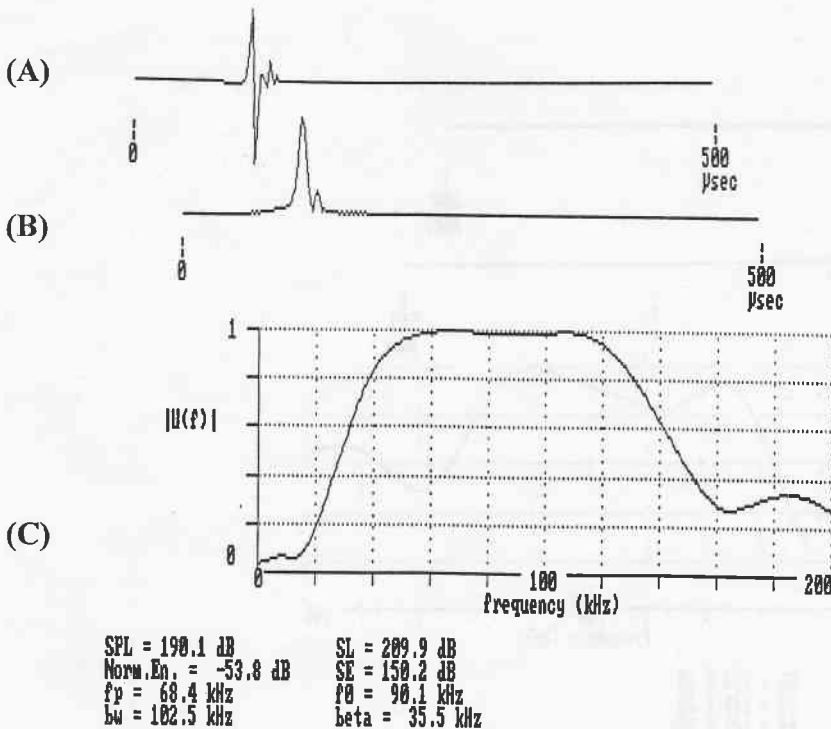


Fig. 7. Normalized time domain waveform $s(t)$ (A), envelope (B), and normalized frequency spectrum $S(f)$ (C) of the spinner dolphin click as it was recorded on the first channel of Fig. 6.

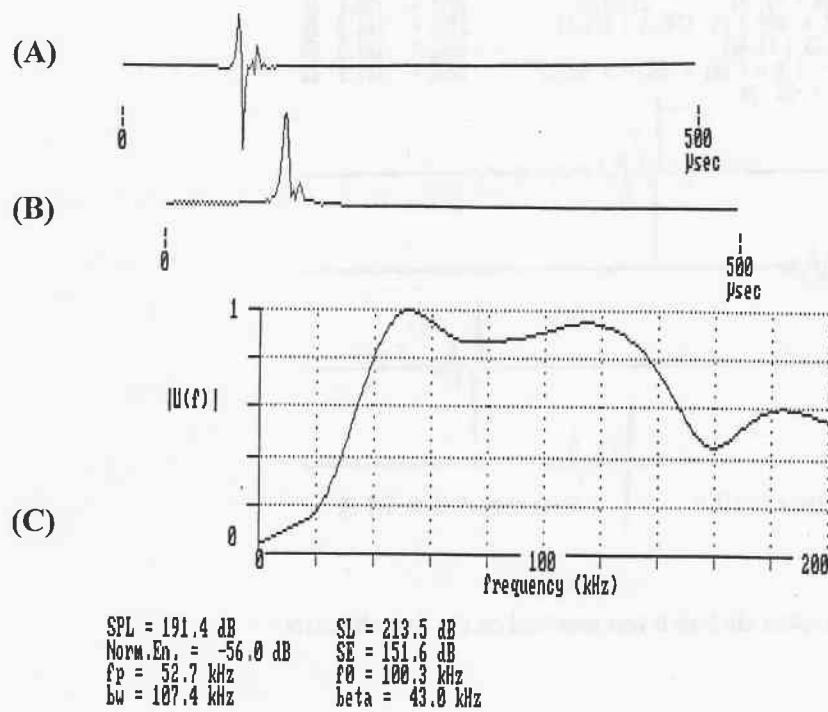


Fig. 8. Normalized time domain waveform $s(t)$ (A), envelope (B), and normalized frequency spectrum $S(f)$ (C) of another spinner dolphin click.

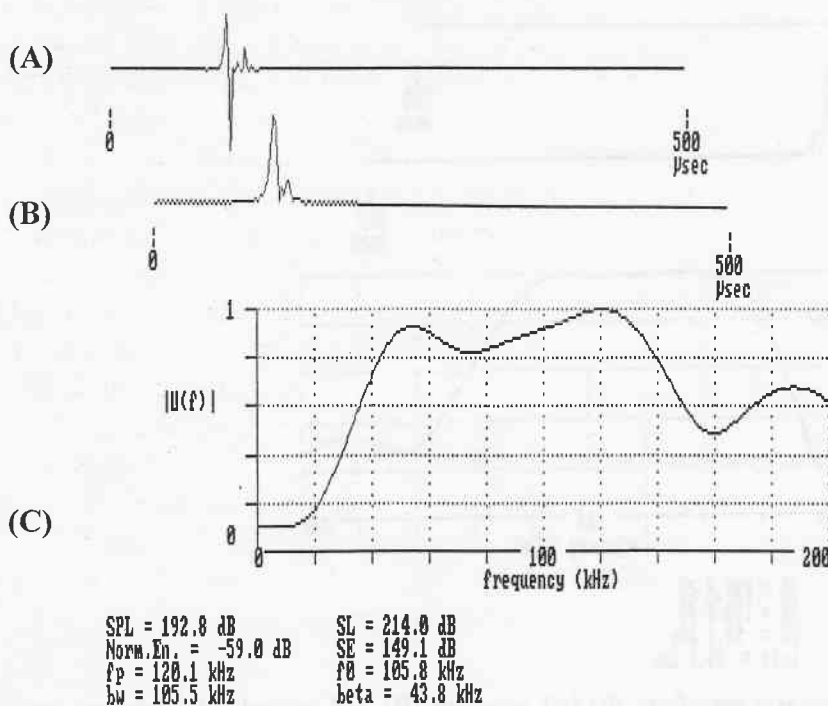


Fig. 9. Normalized time domain waveform $s(t)$ (A), envelope (B), and normalized frequency spectrum $S(f)$ (C) of the next spinner dolphin click in the same click train.

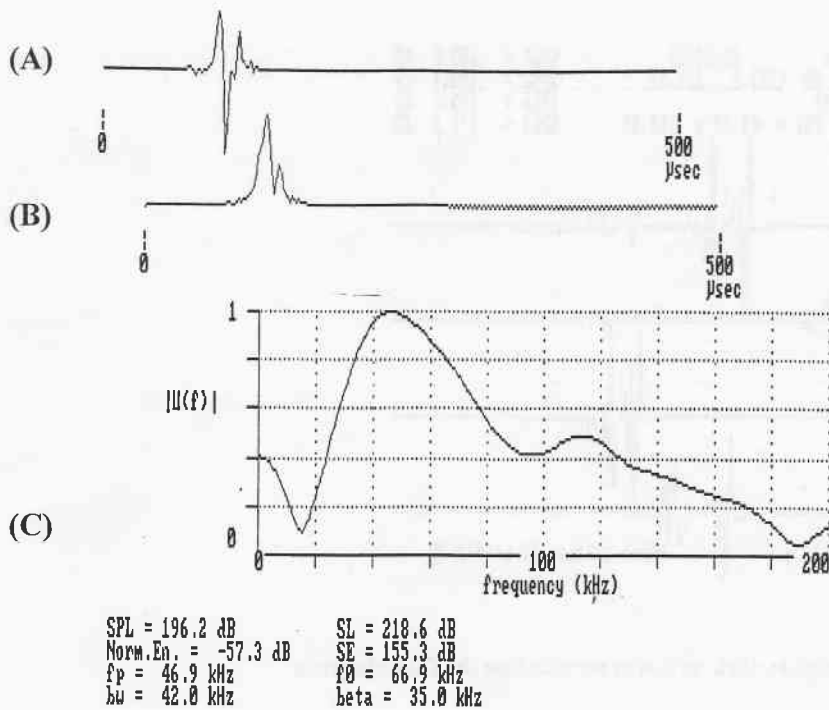


Fig. 10. Normalized time domain waveform $s(t)$ (A), envelope (B), and normalized frequency spectrum $S(f)$ (C) of the spinner dolphin click with the highest recorded source level.

Fig. 11 shows a typical spotted dolphin click as it was received on the four channels, with the highest SPL on the first channel. The actual click was selected by use of the cursor marks (considering the part after the second cursor mark to be surface reflection, for the same reasons as in Fig. 6) and a further click analysis was performed. The waveform, envelope, and spectrum resemble those of the spinner dolphin clicks very much (Fig. 12), although the minor excursions in the time domain were generally higher in amplitude for the spotted dolphin clicks than for the spinner dolphin clicks. The next click from the same spotted dolphin click train (also an H_0 -click) had a waveform, envelope, and spectrum very similar to those of Fig. 12, although unlike Fig. 12 the high frequency peak was somewhat higher in amplitude than the low frequency peak (Fig. 13). Again, the source level was also higher (217.9 versus 217.2 dB for the first click). Other spotted dolphin clicks from the same click train, both of them analyzed on the third channel, had a very broad bandwidth (Fig. 14) and a more unimodal than bimodal spectrum (Fig. 15, with a high source level of 219.3 dB). The click with the highest source level (220.3 dB) of all recorded spotted dolphin clicks, recorded from about 25 m and analyzed on the fourth channel, had a spectrum with an irregular shape (Fig. 16).

In general, spinner dolphin clicks and spotted dolphin clicks were very much alike, although the spotted dolphin clicks seemed to be more variable.

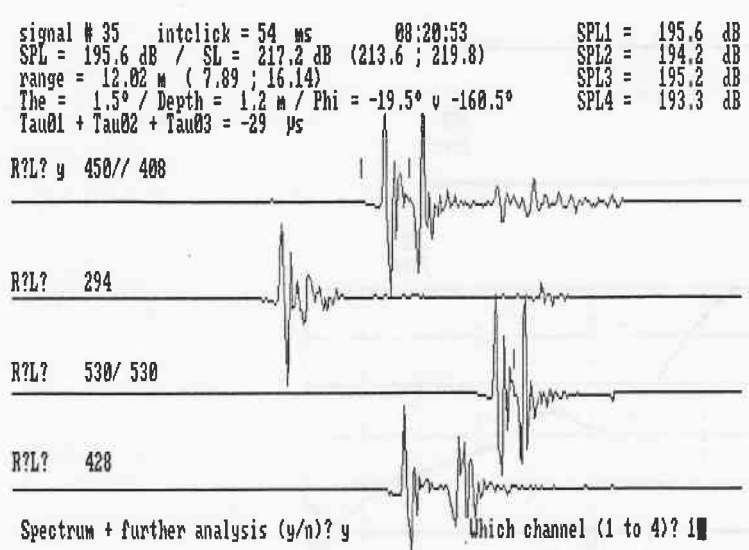


Fig. 11. A single spotted dolphin click as it was received on the four channels.

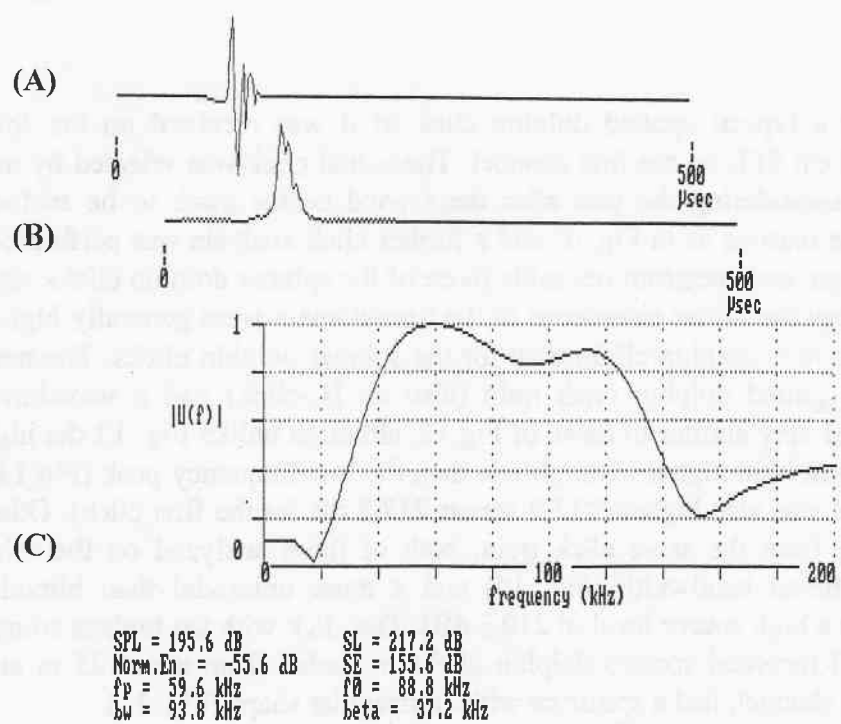


Fig. 12. Normalized time domain waveform $s(t)$ (A), envelope (B), and normalized frequency spectrum $S(f)$ (C) of the spotted dolphin click as it was recorded on the first channel of Fig. 11.

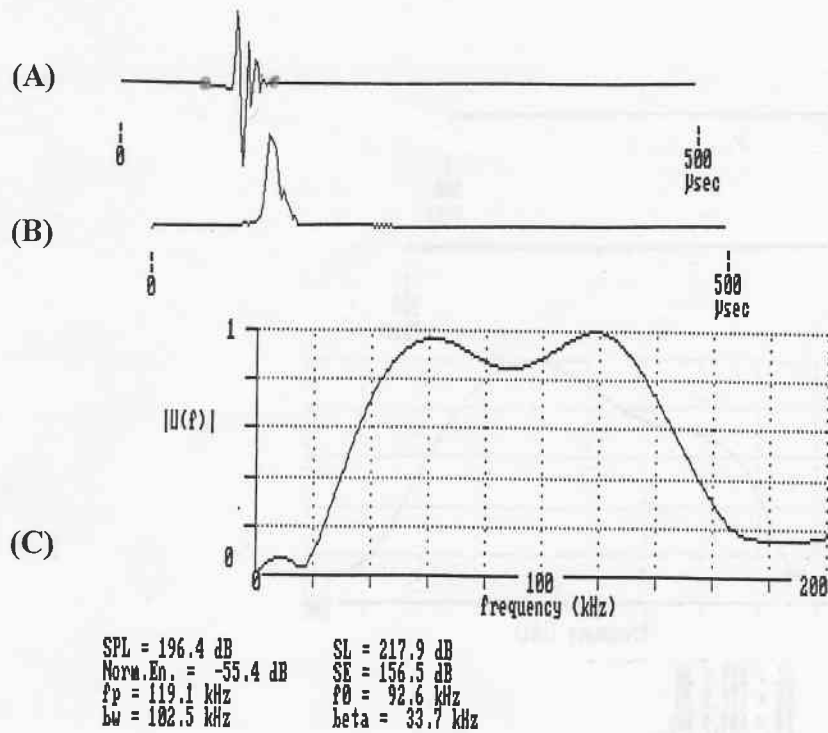


Fig. 13. Normalized time domain waveform $s(t)$ (A), envelope (B), and normalized frequency spectrum $S(f)$ (C) of the next spotted dolphin click in the same click train.

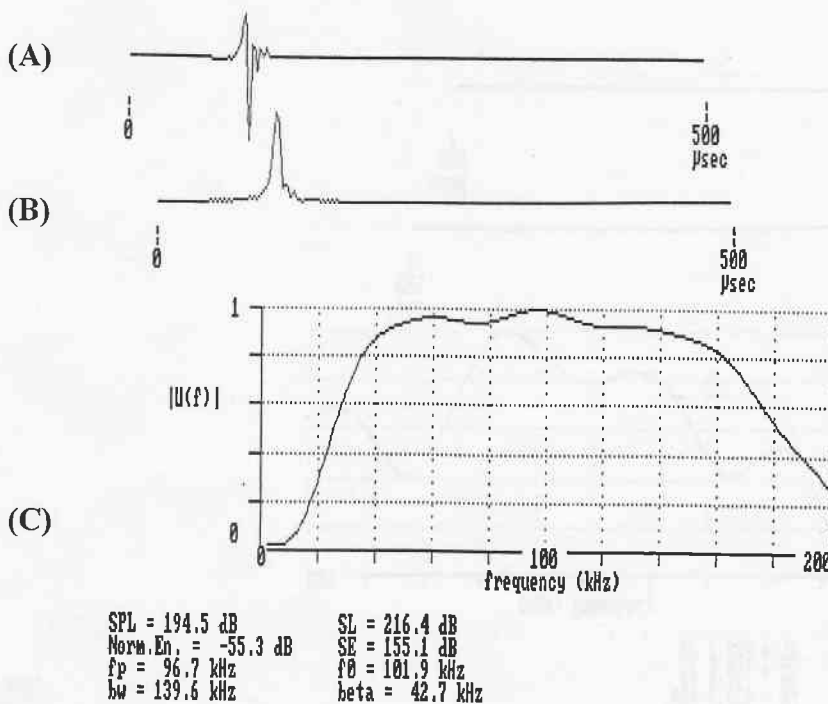


Fig. 14. Normalized time domain waveform $s(t)$ (A), envelope (B), and normalized frequency spectrum $S(f)$ (C) of another spotted dolphin click from the same click train.

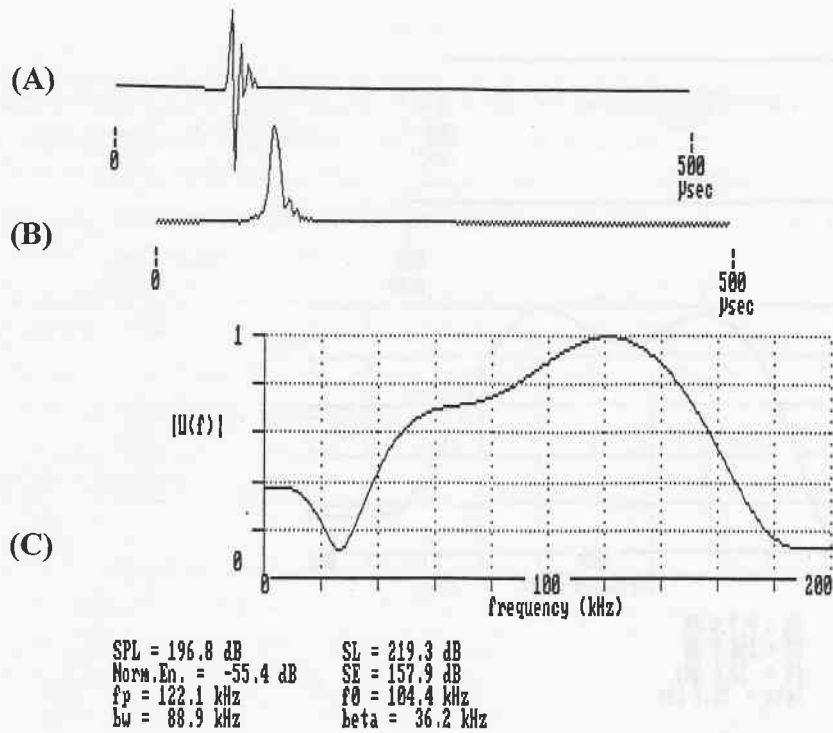


Fig. 15. Normalized time domain waveform $s(t)$ (A), envelope (B), and normalized frequency spectrum $S(f)$ (C) of another spotted dolphin click from the same click train.

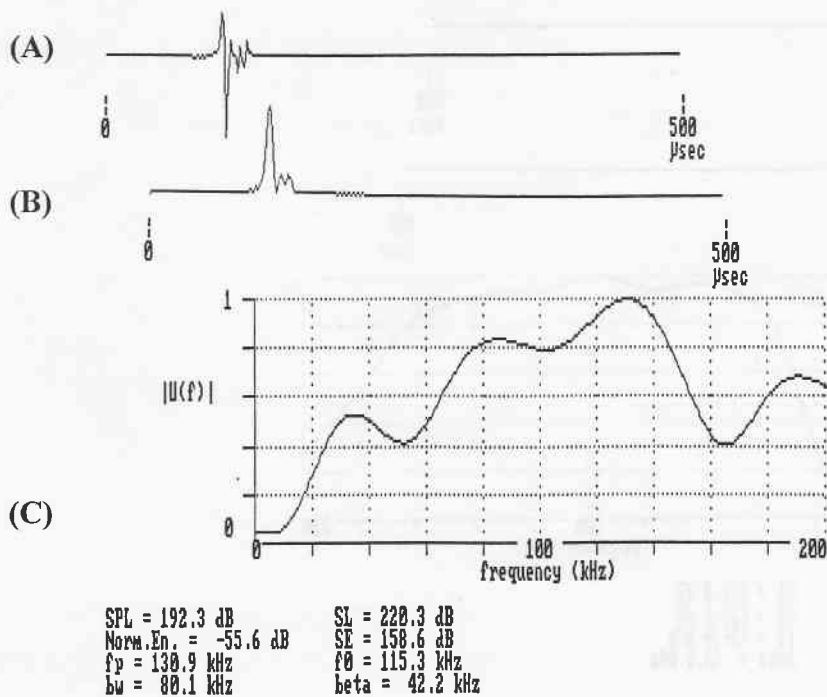


Fig. 16. Normalized time domain waveform $s(t)$ (A), envelope (B), and normalized frequency spectrum $S(f)$ (C) of the spotted dolphin click with the highest recorded source level, from another click train.

Double clicks

Very occasionally, so-called double clicks were recorded (Fig. 17), where a click was followed by a second click 230 or more μs later. The second click was not a case of surface reflection of the first click, nor was it emitted by a different dolphin, because the time delay between the first and second click (332 μs in Fig. 17) was almost identical, with $\pm 2 \mu\text{s}$ accuracy, on all channels on which the second click was recorded. The time delays between the click and its surface reflection on the four channels, Δt_0 , Δt_1 , Δt_2 , and Δt_3 , can be estimated by the equations described earlier and are never identical. Furthermore, the second click is almost identical to the first click in both the time domain (whereas the surface reflection in Fig. 17 is mirrored in amplitude) and in the frequency domain (Fig. 18), on all channels. Because of the narrow beam transmission of clicks, the time and frequency domain of any surface reflection are expected to differ considerably from the actual click.

Note from Fig. 18 that the peak-to-peak sound pressure level, as well as the center frequency and 3-dB bandwidth were higher for the second click than for the first click. This was the case for most recorded double clicks. Although the presented double click was a spotted dolphin click, double clicks were also present within the spinner dolphin clicks. The number of double clicks that were seen within the data probably underestimate the actual number, since second clicks following the first click by more than about 0.5 ms could not be recorded within the 800 μs window.

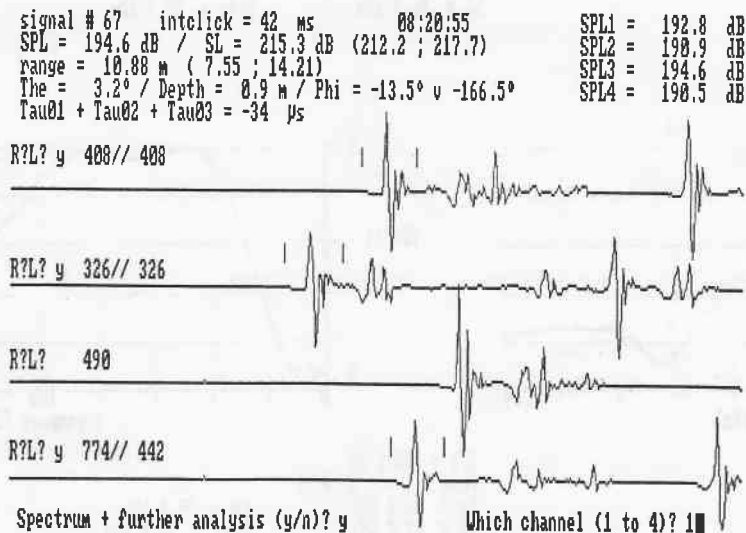
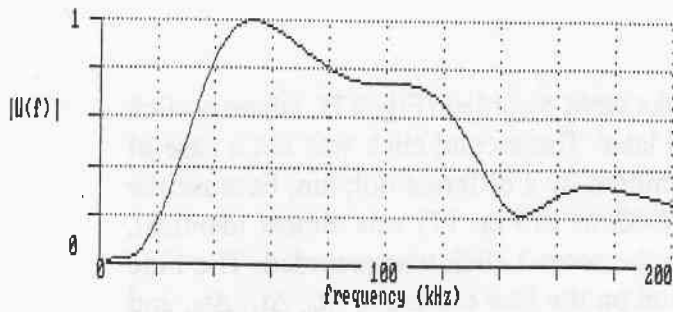
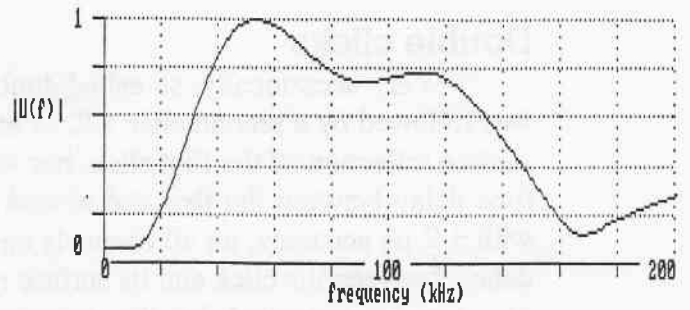


Fig. 17. A spotted dolphin double click as it was received on the four channels. The second click was only recorded on the first, second, and fourth channel.



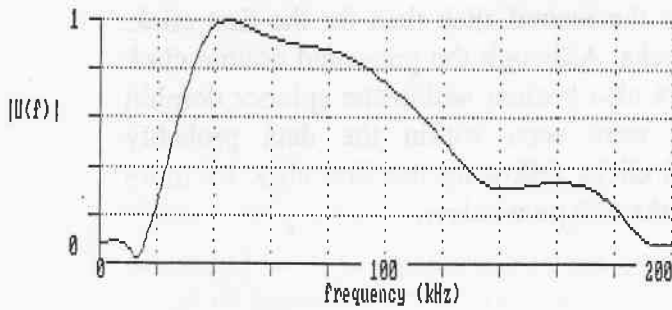
PL = 192.8 dB
 Norm.En. = -55.8 dB
 fp = 53.7 kHz
 w = 81.1 kHz
 SL = 213.5 dB
 SE = 151.7 dB
 f0 = 81.4 kHz
 beta = 36.4 kHz

(A)



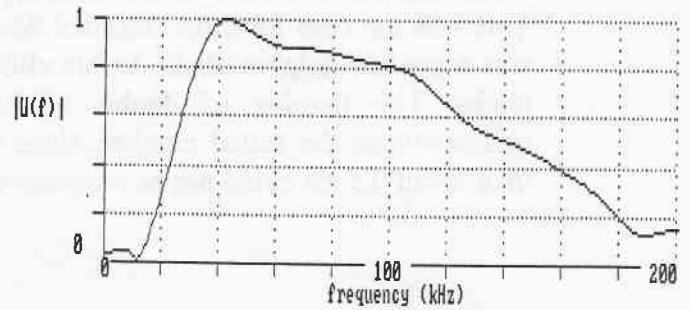
SPL = 192.9 dB
 Norm.En. = -55.6 dB
 fp = 53.7 kHz
 bw = 92.8 kHz
 f0 = 82.5 kHz
 beta = 35.8 kHz

(B)



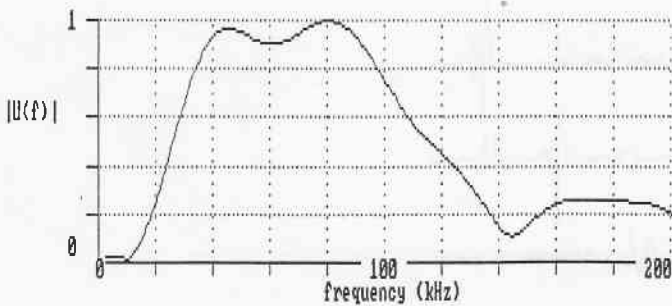
SPL = 190.9 dB
 Norm.En. = -55.6 dB
 fp = 44.9 kHz
 w = 75.2 kHz
 SL = 211.7 dB
 SE = 150.0 dB
 f0 = 75.1 kHz
 beta = 34.1 kHz

(C)



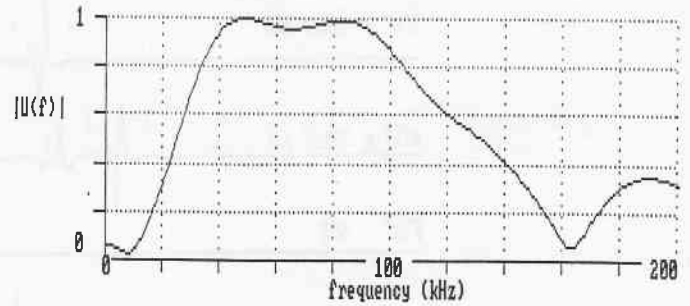
SPL = 191.4 dB
 Norm.En. = -55.3 dB
 fp = 43.9 kHz
 bw = 86.9 kHz
 f0 = 80.9 kHz
 beta = 36.7 kHz

(D)



SPL = 190.5 dB
 Norm.En. = -55.7 dB
 fp = 81.1 kHz
 bw = 73.2 kHz
 SL = 211.3 dB
 SE = 149.5 dB
 f0 = 74.5 kHz
 beta = 32.1 kHz

(E)



SPL = 190.8 dB
 Norm.En. = -55.4 dB
 fp = 48.8 kHz
 bw = 82.0 kHz
 f0 = 79.1 kHz
 beta = 34.9 kHz

(F)

Fig. 18. Normalized frequency spectra of the first (A, C, and E) and second click (B, D, and F) as they were recorded on the first (A and B), second (C and D), and fourth channel (E and F) of Fig. 17.

Characteristics of the spinner and spotted dolphin clicks

After importing all position and click parameters of each click from the channel with the highest SPL into a spreadsheet program, means and standard deviations could be calculated for both species. These are presented in Table I for a number of click characteristics.

Note that the mean peak-to-peak source levels in Table I are only 15 to 20 dB less than the maximum source levels reported by Au (1980) for captive *Tursiops* performing an echolocation task. For the spinner and spotted dolphin clicks, maximum recorded source levels were 222 and 220.3 dB re 1 μ Pa, respectively. Additionally, 3-dB and rms bandwidths were higher than those reported for most odontocete species in literature, while signal durations were shorter. The mean theoretical range resolution values were smaller by about 0.3 cm than the minimum value of 1.0 cm reported for captive *Tursiops* (Au 1993). The minimum range resolution for both the spinner and spotted dolphin clicks was 0.4 cm.

Table I. Summary of a number of signal characteristics ($\bar{X} \pm SD$) for the total sums of clicks of spinner dolphins and spotted dolphins. For the spinner dolphin clicks, sample size $N = 851$, except for SL and SE ($N = 131$), for E_N ($N = 831$), and for f_p ($N = 836$). For the spotted dolphin clicks, $N = 340$, except for SL and SE ($N = 195$), and for f_p ($N = 338$).

	SL(dB)	SE(dB)	E_N (dB)	f_p (kHz)	f_o (kHz)	BW(kHz)	β (kHz)
<i>Stenella longirostris</i>	208.2 \pm 5.4	147.8 \pm 4.7	-57.5 \pm 2.4	69.7 \pm 23.1	80.4 \pm 12.1	76.4 \pm 23.4	34.1 \pm 4.9
<i>Stenella attenuata</i>	211.7 \pm 4.9	150.3 \pm 4.4	-56.9 \pm 1.7	69.4 \pm 31.3	83.4 \pm 16.8	79.8 \pm 35.9	38.7 \pm 6.7
	τ (μ s)	τ_d (μ s)	$\tau_d\beta$	t_0 (μ s)	$\Delta\tau$ (μ s)	Δr (cm)	
<i>Stenella longirostris</i>	31.3 \pm 12.3	4.6 \pm 1.5	0.16 \pm 0.06	11.6 \pm 6.2	9.4 \pm 2.7	0.70 \pm 0.20	
<i>Stenella attenuata</i>	43.1 \pm 15.1	5.3 \pm 1.9	0.21 \pm 0.10	15.8 \pm 8.2	8.9 \pm 3.0	0.67 \pm 0.23	

The mean $\frac{\text{Amb}(300)}{\text{Amb}(0)}$ value (a characteristic that can be used to compare Doppler sensitivity among clicks) was 0.85 (SD = 0.03) for the spinner dolphin clicks and 0.84 (SD = 0.05) for the spotted dolphin clicks (see also the wideband ambiguity diagram of one spinner dolphin click in Fig. 19). For comparison, a digitized typical *Tursiops* click (Fig. 10.3.A from Au 1993) had an $\frac{\text{Amb}(300)}{\text{Amb}(0)}$ of 0.56 while typical signals of *Cephalorhynchus hectori*, *Phocoena phocoena*, and *Phocoenoides dalli* (all belonging to the second acoustic category of odontocetes that was mentioned in the Introduction) had $\frac{\text{Amb}(300)}{\text{Amb}(0)}$ values of 0.28, 0.20, and .016, respectively. Therefore, the spinner and spotted dolphin clicks are even less Doppler sensitive than signals from other odontocete species. However, none of the signals is suitable for resolving target velocities to any useful degree ($\frac{\text{Amb}(20)}{\text{Amb}(0)} \approx 1$ for all six signals, that is, ambiguity densities at $v = 20$ m/s are similar to those at $v = 0$ m/s).

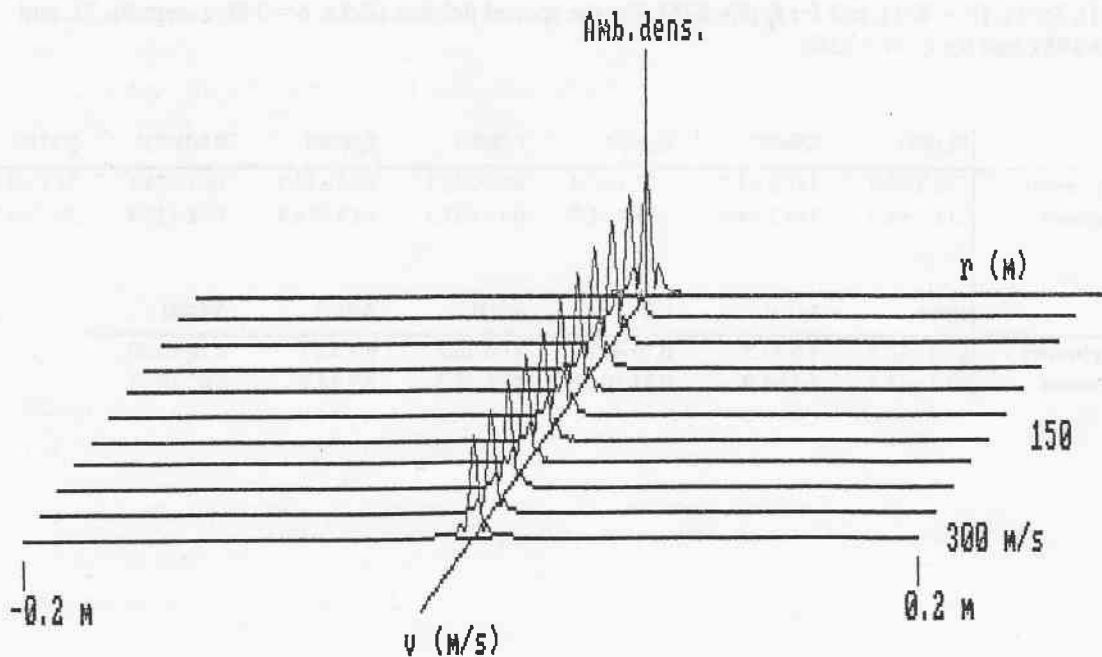


Fig. 19. Wideband ambiguity diagram $\chi(v,r)$ of a spinner dolphin click.

To test for general differences between the spinner and spotted dolphin clicks, each click characteristic in Table I was first subjected to a variance ratio test. Except for SL, SE, and E_N , variances of all click characteristics were significantly higher ($p < 0.0001$) for the spotted dolphin clicks than for the spinner dolphin clicks, thereby confirming the greater variability that was found in the recorded spotted dolphin clicks. Because variances appeared not to be equal, and underlying distributions of click characteristics did not all seem to be normal (see the Appendix), the nonparametric two-tailed Mann-Whitney test, rather than Student's t-test, was used to test for differences between means. It was found that the spotted dolphin clicks had higher values for SL, SE, E_N , f_0 , β , τ , τ_d , $\tau_d\beta$, and t_0 ($p < 0.0001$), while the spinner dolphin clicks had higher values for f_p ($p < 0.05$), $\Delta\tau$, and Δr ($p < 0.0001$). No significant difference in BW was found. Concluding, the recorded spotted dolphin clicks were found to be louder, of longer duration, and with better intrinsic range resolution than the spinner dolphin clicks.

Although spinner dolphin clicks were also found to be recorded from significant larger ranges ($p < 0.0001$) than spotted dolphin clicks, none of the click characteristics of Table I are likely to be related to the position of the dolphin. This was assured by plotting each characteristic separately as a function of range, which resulted in correlation coefficients smaller than 0.2 for all characteristics, except for plotting E_N as a function of range ($r^2 = 0.25$ and 0.27 for the spinner and spotted dolphin clicks, respectively).

Besides the mean values for all recorded clicks presented in Table I, means and standard deviations were also determined for the subselection of all clicks that had the highest SPL recorded by H_0 (H_0 -clicks). However, the Mann-Whitney test showed that, for the spinner dolphin clicks, none of the click characteristics of these H_0 -clicks were significantly different from those presented in Table I. For the spotted dolphin clicks, H_0 -clicks had higher values for f_0 but smaller values for τ and t_0 ($p < 0.05$) than the total sum of clicks. For the remaining click characteristics, no significant differences were found.

Assigning clicks to individual animals

Successive clicks that had similar position parameters were divided into groups, of which each was assumed to be emitted by a single dolphin. By adding the interclick intervals for each group of clicks (except for groups of only one or two clicks), their mean length (\pm SD) could be determined to be 0.83 ± 0.74 s, representing 12.0 ± 9.3 clicks, for the spinner dolphin clicks ($n = 64$ groups), and 0.91 ± 1.06 s, representing 14.1 ± 16.5 clicks, for the spotted dolphin clicks ($n = 23$ groups). The first interclick interval of each group of clicks was not used for this calculation (nor was it used in the further analysis), since these intervals were not part of a click train and only indicate the time between two click trains of different animals.

Next, similar groups of clicks that were separated in time by one or more other groups could be linked and assigned to one animal, taking into account the time between these groups and the animal's direction of movement for each group of clicks. Since two time of arrival differences were already sufficient to divide clicks into groups, it was more convenient to look at time of arrival differences instead of actual positions, in order to assign the large number of recorded clicks that had one channel missing to individual animals as well.

Fig. 20A shows the calculated positions (using only one of the two formulas for ϕ) for 59 clicks that could be localized out of a file of 79 spinner dolphin clicks. Successive clicks that have been grouped together are indicated by identical symbols. The first and last click of each group are connected to the x-y plane by a continuous and dotted line, respectively, from which the direction of movement can be seen. From the positions and direction calculated for each group of clicks (1A, 1B and 1C in Fig. 20A) it has been assumed that they were emitted by the same animal, although this might not be the case. However, since each group of clicks represents one click train in this example, it is highly probable that each group apart has been emitted at least by only one animal. The time elapsed between the last click of group 1A and the first click of 1B was 1 sec and between group 1B and 1C it was 6 sec. Fig. 20B shows the calculated positions for a file of 80 spotted dolphin clicks. Since 0.5 sec elapsed between group 1 and 2 and because of the large distance between them, it is safe to conclude that they were emitted by different animals.

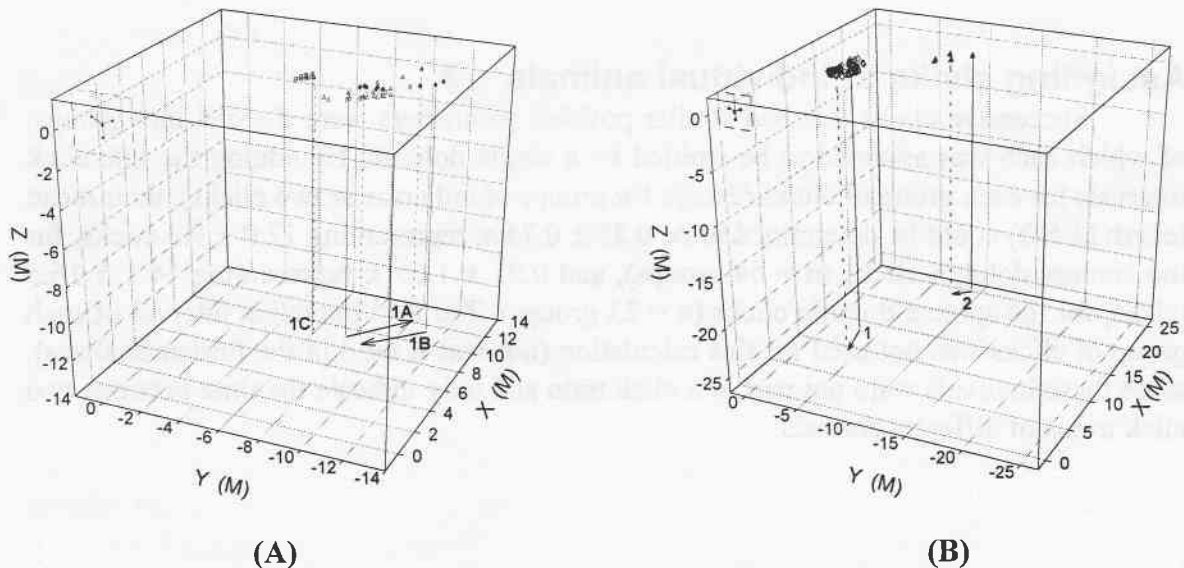


Fig. 20. Calculated positions for click trains 1A, 1B, and 1C emitted by presumably one spinner dolphin (Fig. 20A) and for click trains 1 and 2 emitted by two spotted dolphins (Fig. 20B). Clicks belonging to different click trains are indicated by different symbols. Hydrophone H_0 of the array is at position (0,0,0) and arrows in the x-y plane indicate direction of movement.

After all clicks had been assigned to individual animals, click characteristics were compared among individuals of each species to investigate whether or not the subdivision that was made could be supported additionally by click characteristics other than position parameters of the clicks. This was done by using a method known as discriminant analysis (Lindeman et al. 1980: 183-196, 221), which is essentially similar to a multivariate analysis of variance. A discriminant analysis results in several so-called discriminant functions, each of which assigns weights to all variables fed into the analysis. The variable with the highest absolute weight in the most significant discriminant function is the most important click characteristic to discriminate among individual dolphins.

First, to decide which click characteristics should be fed into the discriminant analysis as variables, preliminary Kruskal-Wallis tests (the nonparametric equivalent of an ANOVA) were performed on all click characteristics, testing one characteristic at a time, to look for differences among individuals. Only individual animals that had three or more clicks been assigned to were tested. All click characteristics were found to differ significantly among the 48 presumed spinner dolphin individuals ($p < 0.0001$) and among the 13 presumed spotted dolphin individuals ($p < 0.05$ for SE, SL, β , and $\frac{Amb(300)}{Amb(0)}$, $p < 0.0001$ for the remaining click characteristics).

Because each click characteristic was found to be significantly different among individuals, ten click characteristics were arbitrarily selected to be fed into the discriminant analysis: E_N , f_p , f_0 , BW, β , τ , τ_d , $\tau_d\beta$, t_0 , and $\Delta\tau$. For the 48 presumed spinner dolphin individuals (representing a total number of 748 clicks), this resulted in nine significant discriminant functions, of which the most important function accounted for 55.0 % of the total variation among individuals. This function assigned the following standardized weights to click characteristics (only indicating proportions of importance):

$$Z_1 = 1.04 \cdot E_N + 0.08 \cdot f_p - 0.07 \cdot f_0 - 0.12 \cdot BW + 0.35 \cdot \beta + 0.16 \cdot \tau + 0.16 \cdot \tau_d + 0.32 \cdot \tau_d\beta + 0.09 \cdot t_0 - 0.30 \cdot \Delta\tau.$$

Using the found discriminant functions, the SPSS program was able to assign 43.9 % of all clicks to the correct individuals. For the 13 presumed spotted dolphin individuals (representing a total number of 335 clicks), the analysis resulted in four significant discriminant functions, of which the most important function accounted for 77.6 % of the total variation among individuals, being:

$$Z_1 = 0.32 \cdot E_N + 0.14 \cdot f_p - 0.98 \cdot f_0 - 0.02 \cdot BW + 0.73 \cdot \beta + 0.99 \cdot \tau + 0.57 \cdot \tau_d - 0.77 \cdot \tau_d\beta - 0.31 \cdot t_0 - 0.61 \cdot \Delta\tau.$$

Using the calculated functions, 39.7 % of the clicks could be assigned to the correct spotted dolphin individuals. If a discriminant analysis was applied to the selection of only H_0 -clicks, eight significant discriminant functions were found for the spinner dolphins (assigning 56.3 % of the clicks correctly) and two significant functions for the spotted dolphins (assigning 79.7 % of the clicks correctly).

It should be noted that either omitting characteristics from the analyses, or adding new characteristics to them, resulted in quite different discriminant functions than the ones described above. Therefore, the exact meaning of the weights that were assigned to click characteristics is ambiguous. In all cases, however, one or more significant discriminant functions were obtained, thus supporting the assignment of clicks to individual animals that was made.

Click trains of a spinner and a spotted dolphin

For three click trains of a spinner dolphin and one long train of a spotted dolphin (of which the calculated positions are shown in Fig. 20A and 20B, respectively), the means and standard deviations of their click characteristics are presented in Table II. Variance ratio tests showed that the variances of all click characteristics were significantly higher ($p < 0.0001$) for the spotted dolphin than for the spinner dolphin. Furthermore, using the Mann-Whitney test, it was found that the spotted dolphin click train had higher values for SL, SE, β , τ , τ_d , and $\tau_d\beta$ ($p < 0.0001$), while the spinner dolphin trains had higher values for E_N ($p < 0.0001$), f_p , $\Delta\tau$, and Δr ($p < 0.05$). No significant differences in f_0 , BW, and t_0 were found. Ranges from which the spinner and spotted dolphin click trains were recorded were not significantly different either.

Table II. Summary of a number of signal characteristics ($\bar{X} \pm SD$) for the click trains of the individual spinner dolphin and spotted dolphin. For the spinner dolphin clicks, sample size $N = 74$, except for SL, SE, and E_N ($N = 59$). For the spotted dolphin clicks, $N = 75$.

	SL(dB)	SE(dB)	E_N (dB)	f_p (kHz)	f_0 (kHz)	BW(kHz)	β (kHz)
<i>S. longirostris</i> (1 ind.)	205.8 \pm 3.2	147.9 \pm 2.8	-52.7 \pm 0.8	68.1 \pm 18.2	75.7 \pm 11.1	79.7 \pm 19.8	31.4 \pm 2.9
<i>S. attenuata</i> (1 ind.)	211.5 \pm 5.6	150.3 \pm 5.0	-56.5 \pm 1.4	62.4 \pm 30	79.1 \pm 16.6	73.4 \pm 37.0	39.6 \pm 8.2
	τ (μ s)	τ_d (μ s)	$\tau_d\beta$	t_0 (μ s)	$\Delta\tau$ (μ s)	Δr (cm)	
<i>S. longirostris</i> (1 ind.)	30.3 \pm 6.7	4 \pm 1.2	0.13 \pm 0.04	16.5 \pm 5.2	9.8 \pm 2.5	0.73 \pm 0.19	
<i>S. attenuata</i> (1 ind.)	43.7 \pm 10.6	5.8 \pm 2	0.23 \pm 0.11	17.8 \pm 8.1	9.6 \pm 3.2	0.72 \pm 0.24	

Additionally, several click characteristics were plotted as a function of click number. Fig. 21 shows the interclick intervals for both animals, which started off high, fluctuated throughout each train in a cyclic manner and ended at a lower value, but were always higher than the so-called two-way transit time. This is the time needed for an echolocation click to travel from the dolphin to the target and then return as an echo to the dolphin, and can be expressed as $2R/c$, with $c \approx 1500$ m/s and R being the calculated distance from the dolphin to the array.

Peak-to-peak source levels and source energies of the same click trains are presented in Fig. 22. Since the first 15 clicks of the spinner dolphin's second recorded click train were not recorded on the third channel, no ranges and therefore no values for SL and SE could be calculated for those clicks. SL and SE show similar although not identical fluctuations, generally starting and ending at lower values than the clicks in the middle part of each train. The spotted dolphin reached a maximum SL of 219.8 dB re 1 μ Pa, which is 9.1 dB higher than the highest spinner dolphin's click. The spotted dolphin's click train also shows a much larger variation than the spinner dolphin's trains.

Additionally, center frequencies and rms bandwidths were more variable and reached higher maximum values for the spotted dolphin than for the spinner dolphin (Fig. 23). For both dolphins f_0 was always higher than β , with both click characteristics showing similar fluctuations and f_0 having the biggest variation. Peak frequencies and 3-dB bandwidths on the other hand followed very much the same patterns, with sometimes f_p being higher than BW but in most cases higher BWs (Fig. 24). Again, the spotted dolphin reached higher maximum values and showed more variation. Peak frequencies, center frequencies and 3-dB bandwidths generally seem to start off low, increase during the click train and then decrease again at the end (in contrast to the relatively steady rms bandwidths). This is reflected in the theoretical range resolution properties of the clicks, with poor resolution at the beginnings and endings of click trains, and better resolution values in the middle regions (Fig. 25). The spotted dolphin clicks reached lower and therefore better resolution values, but showed more variation than the spinner dolphin clicks. The spinner dolphin clicks, however, had lower time bandwidth products and therefore approximated the Gabor elementary signal more closely. Signal durations, finally, were shorter for the spinner dolphin clicks and showed less variation, with respect to rms durations, than for the spotted dolphin clicks (Fig. 26).

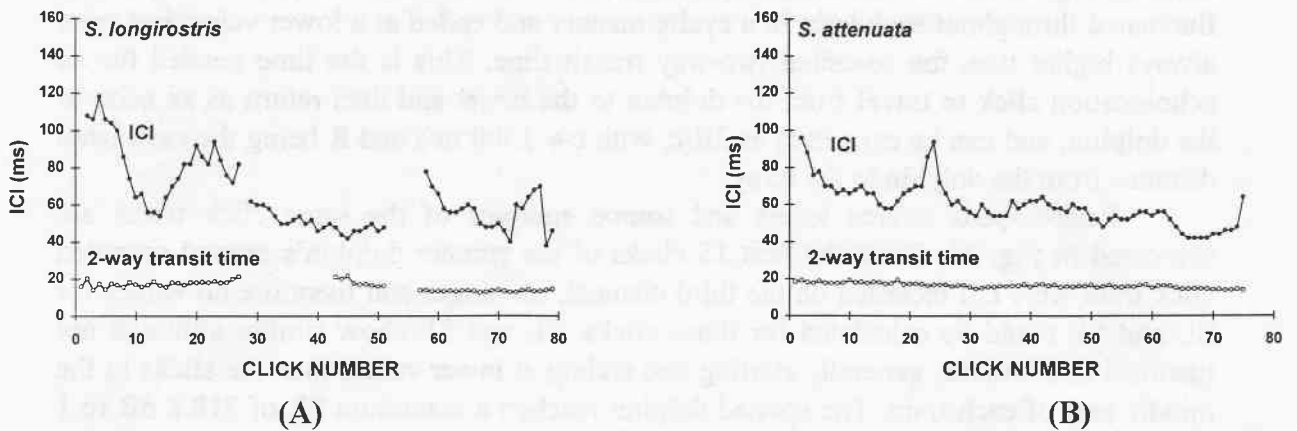


Fig. 21. Interclick intervals and 2-way transit times for the three spinner dolphin click trains (A) and one spotted dolphin click train (B).

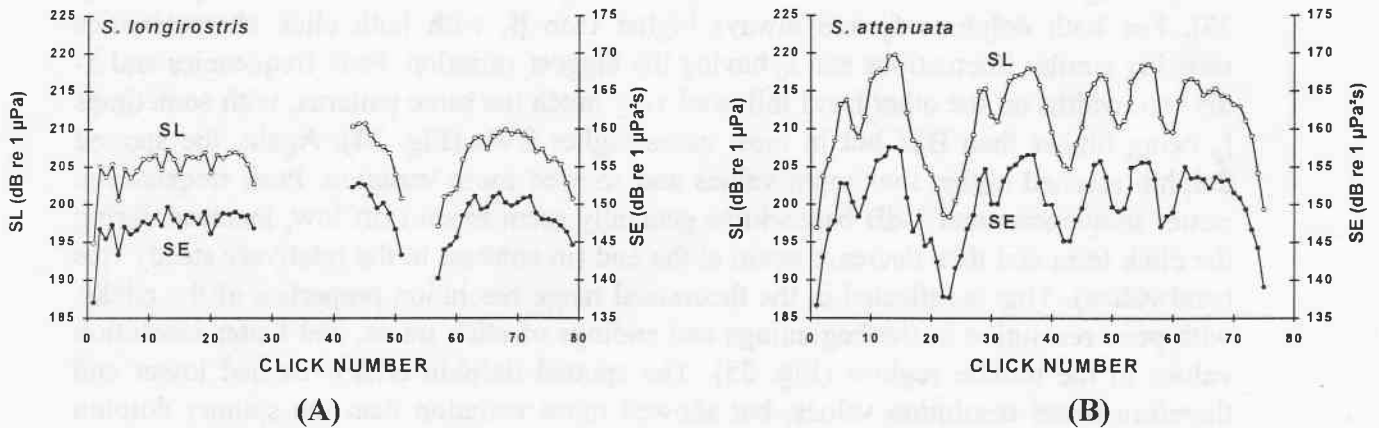


Fig. 22. Source levels and source energies for the three spinner dolphin click trains (A) and one spotted dolphin click train (B).

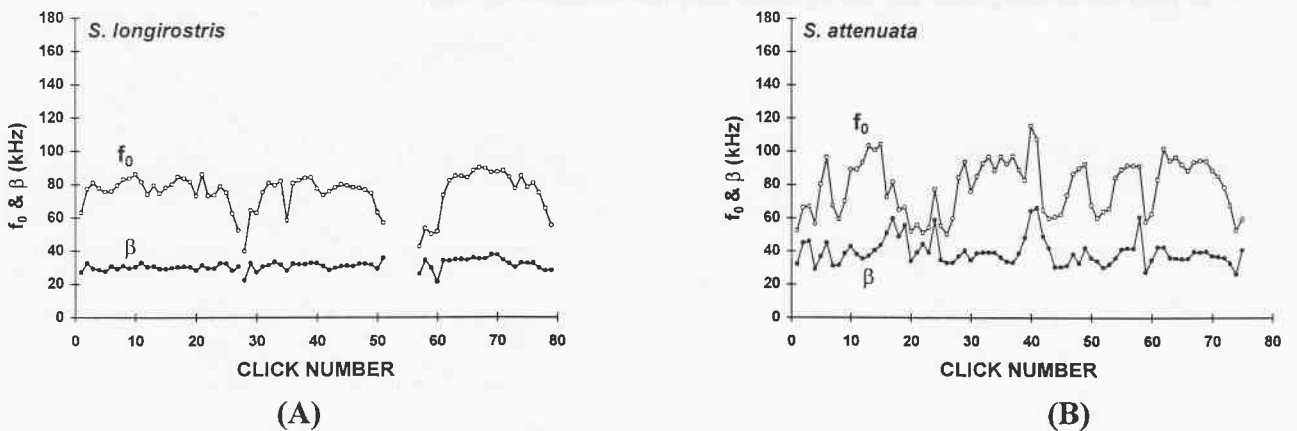
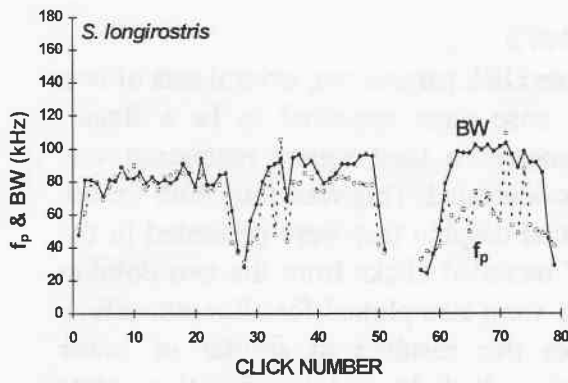
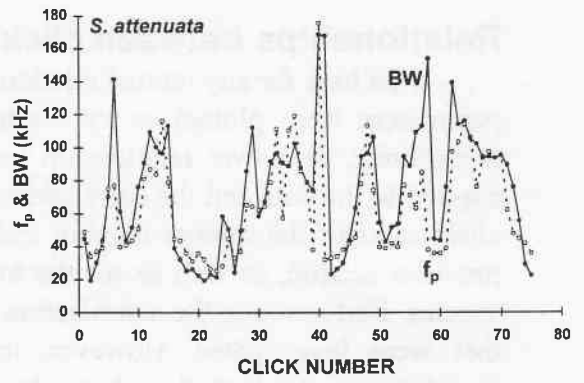


Fig. 23. Center frequencies and rms bandwidths for the three spinner dolphin click trains (A) and one spotted dolphin click train (B).

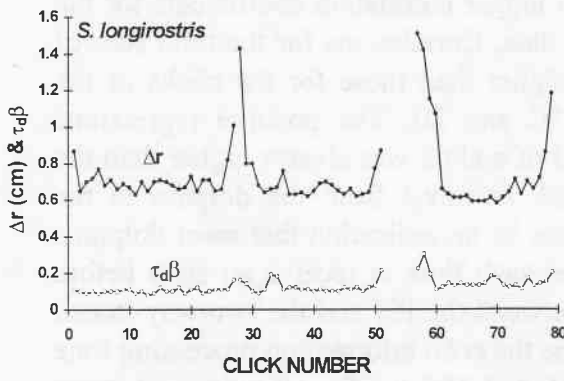


(A)

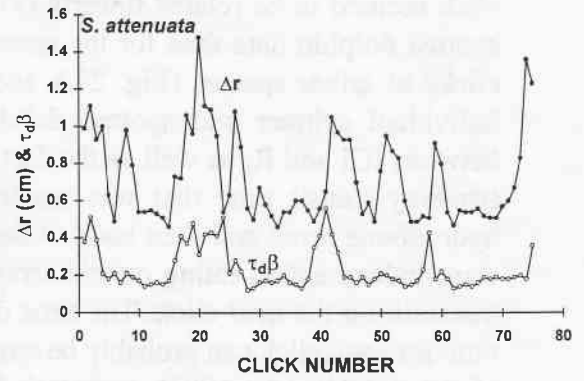


(B)

Fig. 24. Peak frequencies and 3-dB bandwidths for the three spinner dolphin click trains (A) and one spotted dolphin click train (B).

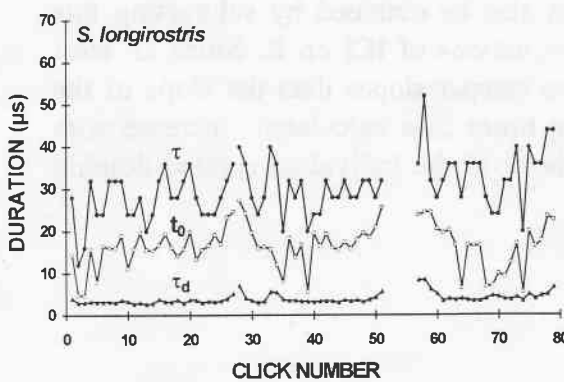


(A)

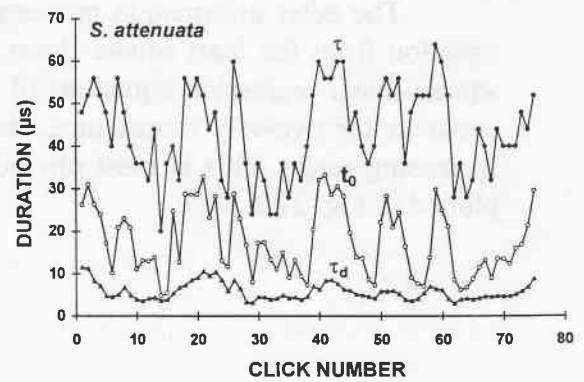


(B)

Fig. 25. Range resolution and time bandwidth product for the three spinner dolphin click trains (A) and one spotted dolphin click train (B).



(A)



(B)

Fig. 26. Signal duration, centroid of the time domain and rms signal duration for the three spinner dolphin click trains (A) and one spotted dolphin click train (B).

Relationships between click parameters

To look for any mutual relationships between click parameters, several sets of two parameters were plotted as xy scatter plots. In case there appeared to be a linear, logarithmic, or power relationship between parameters, a least square regression was applied to the data and the correlation coefficient calculated. This was done both for the click trains of the spinner dolphin and of the spotted dolphin that were presented in the previous section, as well as for the total sums of recorded clicks from the two dolphin species. Furthermore, the subselection of H_0 -clicks were also plotted for all relationships that were investigated. However, in most cases this resulted in similar or lower correlation coefficients than those obtained by plotting all clicks, and therefore these plots are not presented.

1. *Interclick interval versus range*

Interclick intervals and the corresponding ranges that were calculated for each click seemed to be related linearly (Fig. 27), with higher correlation coefficients for the spotted dolphin data than for the spinner dolphin data. Correlations for the total sum of clicks of either species (Fig. 27A and B) were higher than those for the clicks of the individual spinner and spotted dolphin (Fig. 27C and D). The positive regressions between ICI and R, as well as the fact that the ICI of a click was always higher than the two-way transit time that was needed for a click to travel from the dolphin to the hydrophone array and then back to the dolphin, can be an indication that most dolphins were indeed echolocating on the array and waited each time to receive an echo before transmitting the next click. The time difference between the ICI and the two-way transit time for each click can probably be considered to be the echo information processing time of the dolphin (Au 1993), and varied between 16 and 105 ms for all spinner dolphin clicks ($\bar{x} = 48.9$, $SD = 22.2$, $n = 114$), and between 27 and 93 ms for all spotted dolphin clicks ($\bar{x} = 44.9$, $SD = 12.3$, $n = 171$). In Fig. 20, the equation of the two-way transit time as a function of range is also plotted and can be expressed as:

$$\text{2-way transit time (ms)} = 1.33 * R \text{ (m)}.$$

The echo information processing time can also be obtained by subtracting this equation from the least square linear regression equations of ICI on R. Since all least square linear regression equations of Fig. 27 have steeper slopes than the slope of the equation for two-way transit time, the processing times thus calculated increase with increasing range. This is most obvious for the clicks of the individual spotted dolphin plotted in Fig. 27D.

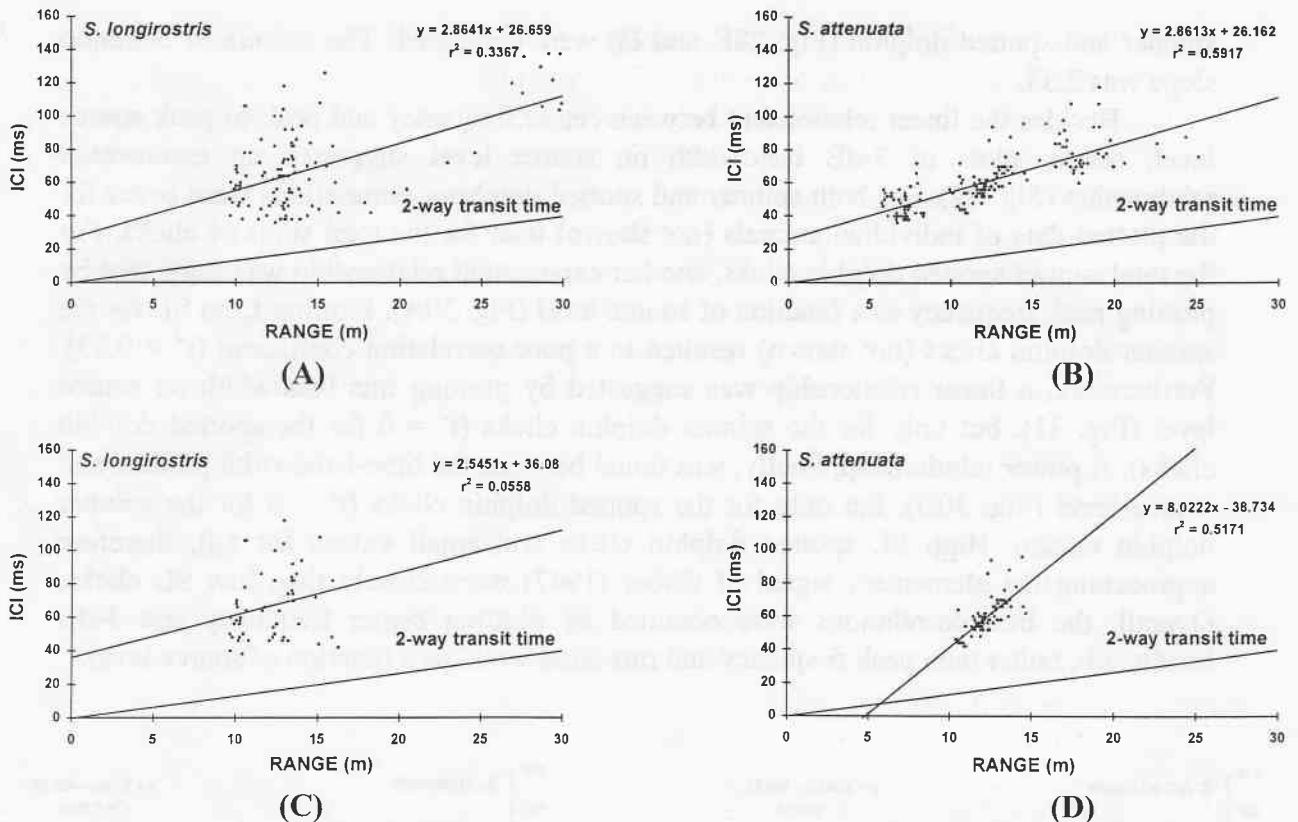


Fig. 27. Scatter plots of interclick interval on range for the total sum of spinner dolphin clicks (A) and the total sum of spotted dolphin clicks (B), and for the click trains of the individual spinner dolphin (C) and individual spotted dolphin (D). The equation of the least square linear regression line through the data and its correlation coefficient are indicated in the upper right corner of each plot.

2. Center frequency and 3-dB bandwidth versus peak-to-peak source level

As found earlier by Au *et al.* (1995) for a false killer whale, *Pseudorca crassidens*, center frequency seems to be related linearly to peak-to-peak source level for the spinner and spotted dolphin clicks too (Fig. 28). Only source levels derived from unsaturated sound pressure levels (i.e., only SPLs that could be fully captured by the data acquisition boards) were plotted in Fig. 28, since the SL of saturated signals would be an underestimation of their real SL. The four plots of Fig. 28 (plotted click trains of one animal and total sum of clicks for spinner as well as spotted dolphins) have similar correlation coefficients and similar least square linear regression equations, that also approach the equation (f_0 (kHz) = 2.55 · SL (dB) - 456.40) found by Au *et al.* (1995). Because of this similarity, the linear regression equations were compared between spinner and spotted dolphins using Student's t-test in the way described by Zar (1984: 292-305). The slopes of the linear regression equations for the total sums of clicks of either spinner or spotted dolphins (Fig. 28A and B) were found not to be significantly different from each other ($p > 0.5$). Therefore, a common slope could be calculated, which was 2.35. However, the elevations of the two equations were found to be significantly different ($p < 0.001$). The same results were obtained (no significantly different slopes by $p > 0.5$, but different elevations by $p < 0.001$) if the linear regression equations for the individual

spinner and spotted dolphin (Fig. 28C and D) were compared. The calculated common slope was 2.33.

Besides the linear relationship between center frequency and peak-to-peak source level, scatter plots of 3-dB bandwidth on source level suggested an exponential relationship (Fig. 29). For both spinner and spotted dolphins, correlations were better for the plotted data of individual animals (not shown) than for the total sums of clicks. For the total sum of spotted dolphin clicks, another exponential relationship was suggested by plotting peak frequency as a function of source level (Fig. 30A). Plotting f_p on SL for the spinner dolphin clicks (not shown) resulted in a poor correlation coefficient ($r^2 = 0.23$). Furthermore, a linear relationship was suggested by plotting rms bandwidth on source level (Fig. 31), but only for the spinner dolphin clicks ($r^2 = 0$ for the spotted dolphin clicks). A power relationship, finally, was found between the time-bandwidth product and source level (Fig. 30B), but only for the spotted dolphin clicks ($r^2 = 0$ for the spinner dolphin clicks). High SL spotted dolphin clicks had small values for $\tau_d\beta$, therefore approaching the elementary signal of Gabor (1947) more closely than low SL clicks. Overall, the best correlations were obtained by plotting center frequency and 3-dB bandwidth, rather than peak frequency and rms bandwidth, as a function of source level.

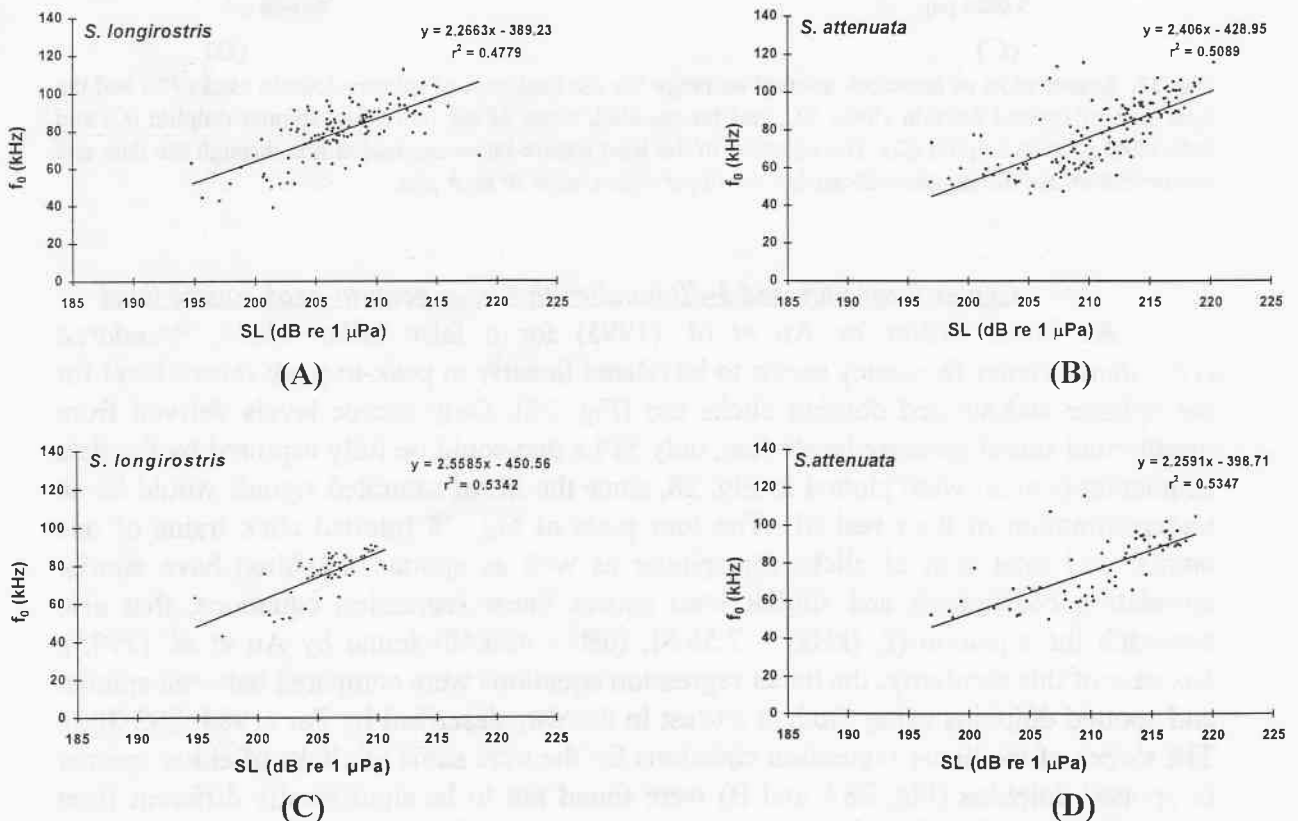
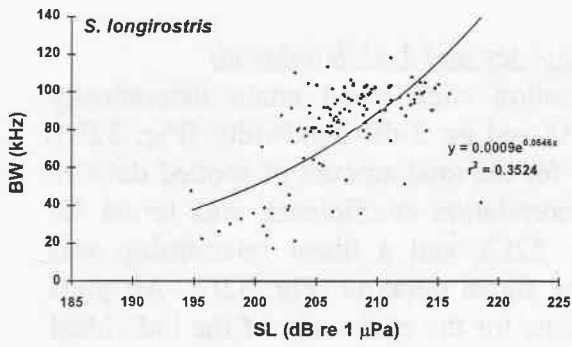
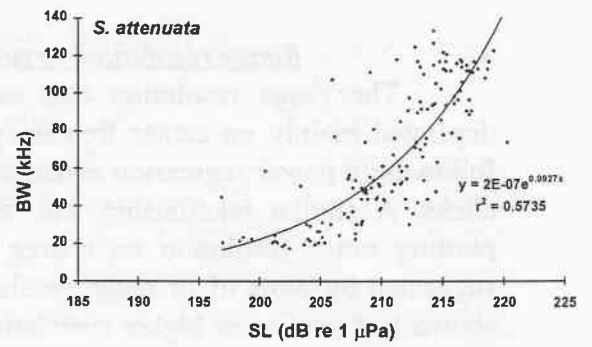


Fig. 28. Scatter plots of center frequency on peak-to-peak source level for the total sum of spinner dolphin clicks (A) and the total sum of spotted dolphin clicks (B), and for the click trains of the individual spinner dolphin (C) and individual spotted dolphin (D). The equation of the least square linear regression line through the data and its correlation coefficient are indicated in the upper right corner of each plot.

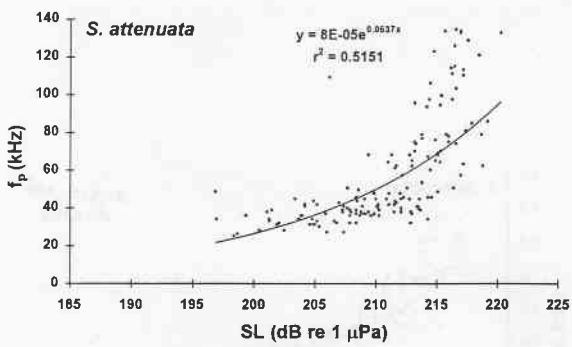


(A)

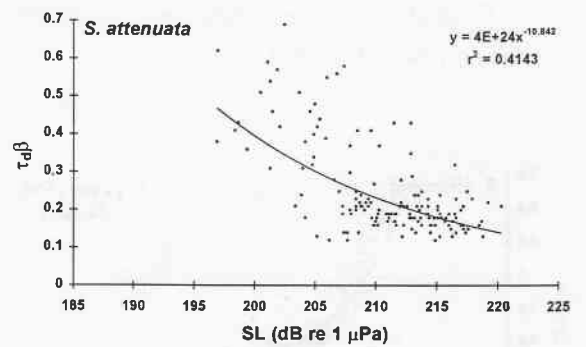


(B)

Fig. 29. Scatter plots of 3-dB bandwidth on peak-to-peak source level for the total sum of spinner dolphin clicks (A) and the total sum of spotted dolphin clicks (B).



(A)



(B)

Fig. 30. Scatter plots of peak frequency on source level (A) and time bandwidth product on source level (B) for the total sum of spotted dolphin clicks.

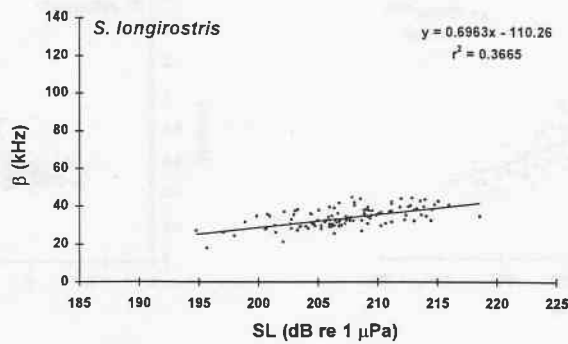


Fig. 31. Scatter plot of rms bandwidth on source level for the total sum of spinner dolphin clicks.

3. Range resolution versus center frequency and 3-dB bandwidth

The range resolution that each echolocation click could attain theoretically depended mainly on center frequency (Fig. 32A) and on 3-dB bandwidth (Fig. 32B), following a power regression equation as shown for the total amount of spotted dolphin clicks. A similar relationship, but with lower correlation coefficients, was found for plotting range resolution on source level (Fig. 32C), and a linear relationship was suggested by plots of of range resolution on rms signal duration (Fig. 32D). All plots shown had similar or higher correlation coefficients for the click train of the individual spotted dolphin (not shown) than for the total amount of spotted dolphin clicks. All relationships shown were also found for the spinner dolphin clicks (not shown either). Generally, short duration, high amplitude clicks with high frequencies and broad bandwidths had the best intrinsic resolutions.

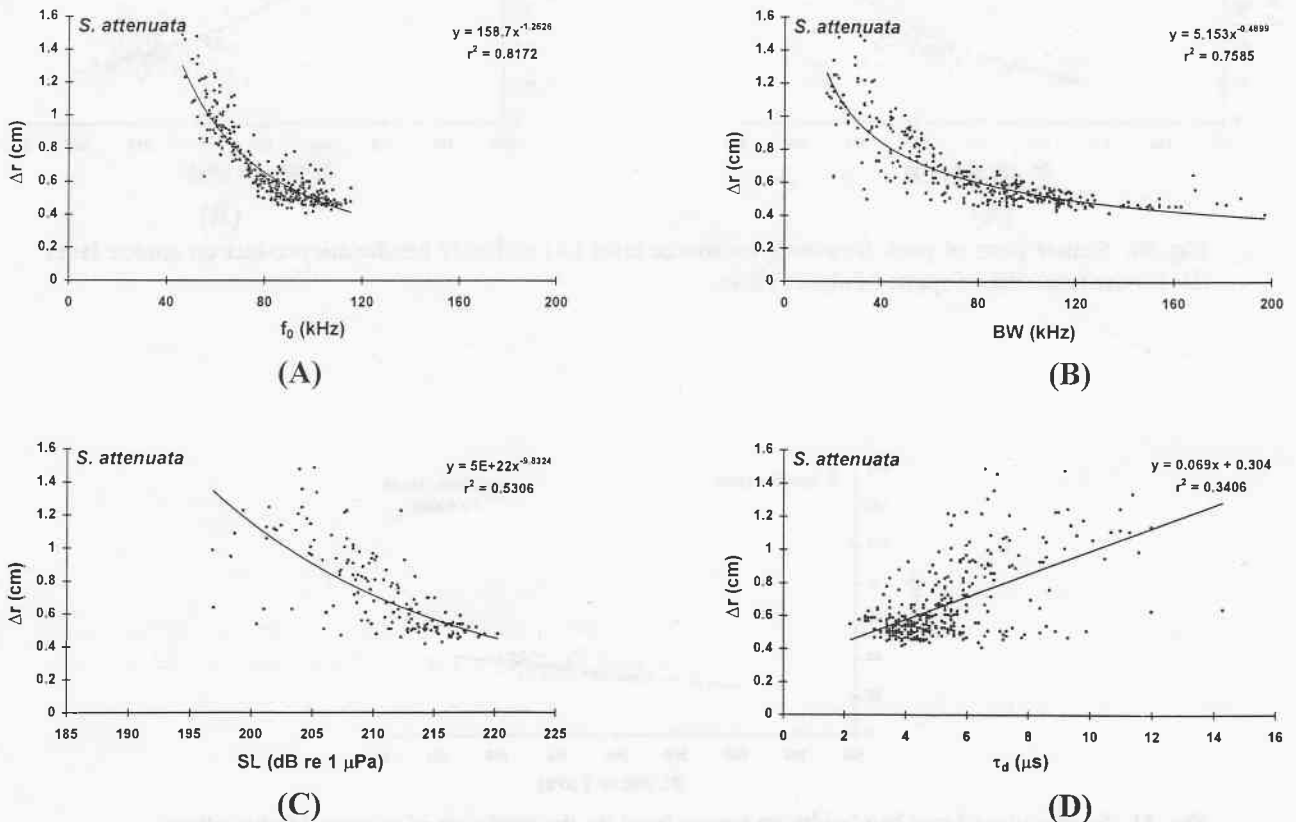


Fig. 32. Scatter plots of the theoretical range resolution values of the total sum of spotted dolphin clicks as a function of center frequency (A), 3-dB bandwidth (B), peak-to-peak source level (C), and rms duration (D).

4. 3-dB bandwidth versus center frequency

Scatter plots of 3-dB bandwidth on center frequency suggested a positive linear relationship (Fig. 33). The plotted clicks of the individual spinner and spotted dolphin (Fig. 33C and D) had higher correlation coefficients than plots of the total sum of clicks of either species (Fig. 33A and B). Furthermore, plots of 3-dB bandwidth on peak frequency also suggested a positive but weaker relationship (Fig. 34), with power regressions giving slightly higher correlation coefficients than linear regressions.

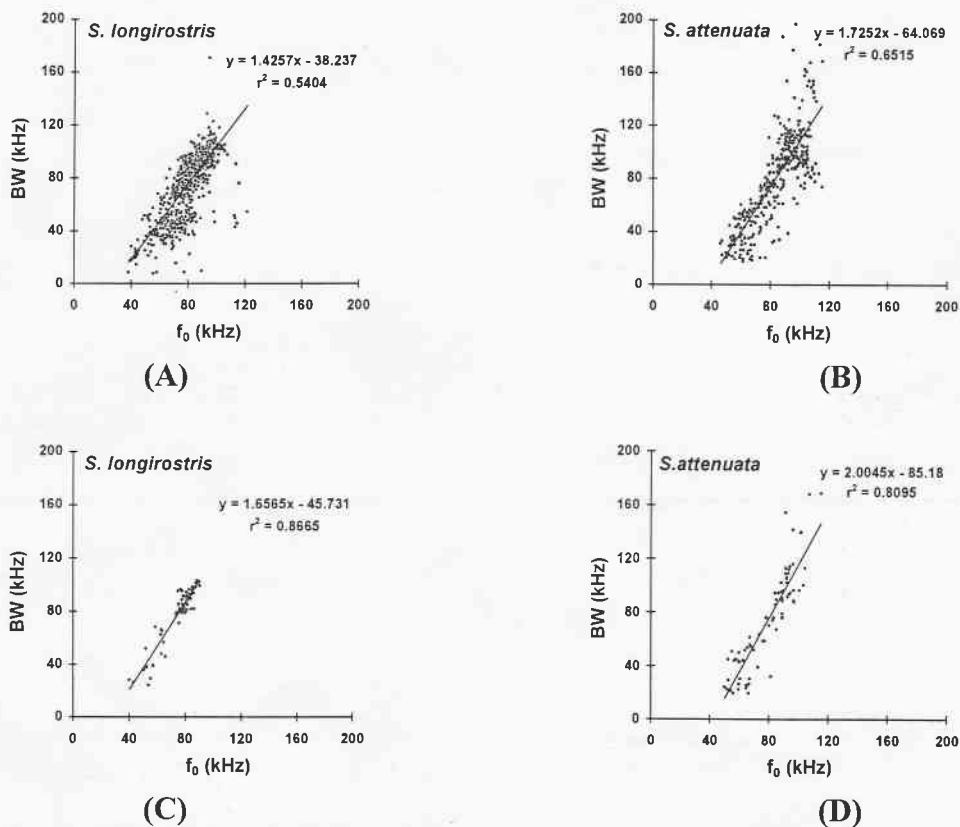
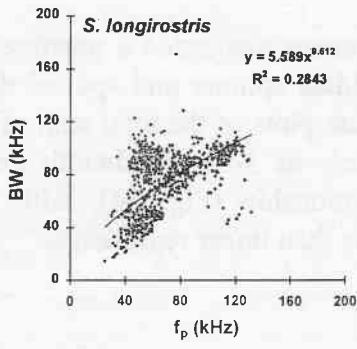
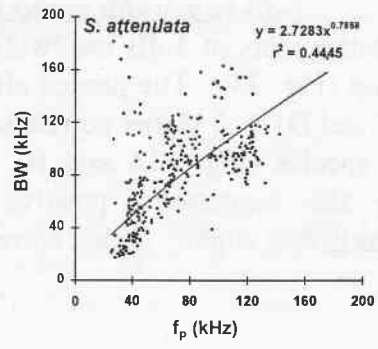


Fig. 33. Scatter plots of 3-dB bandwidth on center frequency for the total sum of spinner dolphin clicks (A) and total sum of spotted dolphin clicks (B), and for the click trains of the individual spinner dolphin (C) and individual spotted dolphin (D).



(A)



(B)

Fig. 34. Scatter plots of 3-dB bandwidth on peak frequency for the total sum of spinner dolphin clicks (A) and the total sum of spotted dolphin clicks (B).

DISCUSSION & CONCLUSIONS

Type of array and method of localizing

The results of the range calibration of the four hydrophone symmetrical star array, as well as the succeeded video recordings from two captive *Tursiops* echolocating on the array, show that the use of this type of array can be highly accurate to localize dolphins transmitting clicks from ranges up to 15 m, and sufficiently accurate from ranges up to 25 m. For theoretical reasons, ranges larger than 30 m cannot be estimated with any accuracy, at least for the size of the used array (with a distance a between the center hydrophone and outer hydrophones of 0.61 m).

Measuring ranges larger than 30 m would only be possible by using a larger-sized array. However, one of the disadvantages of a larger array (regardless of it being less manageable) are increased time of arrival differences, so that more digitized points at each channel would be needed to store the clicks. Because there has to be made a trade-off for each data acquisition board between the number of digitized points stored for each recorded click and the number of clicks that can be stored successively into one file, this would mean that less successive clicks can be stored each time. Furthermore, a larger-sized array would not record echolocation clicks on all four channels from animals at small ranges (and therefore excluding the possibility of localizing them) because of the narrow transmission beam pattern of dolphin echolocation clicks. A third disadvantage of a larger array would be the increased chance of recording multiple clicks, transmitted simultaneously by different animals, on different channels. Therefore, both the size and type of the hydrophone array that was used are very suitable for accurately localizing dolphins at ranges up to 25 m, using their echolocation clicks.

The method that was used to determine the time of arrival differences (taking the maximum positive peak of the recorded click as time of click arrival at each channel, in combination with the 3-point parabolic curve fit to estimate the exact peak in between digitized points) resulted in the smallest range estimation errors when applied to the calibration results. Other methods, such as taking both positive and negative peaks instead of only positive peaks, or using a 5-point parabolic curve fit instead of a 3-point curve fit, proved to be less accurate. Methods that have been used in the past to determine time of arrival differences include taking the peak of the click envelope (Møhl et al. 1990) or taking the peak of the sonagram (frequency versus time plot) as time of signal arrival at each channel, as reported by Magyar et al. (1978) for bird song. Both methods require a mathematical transformation of the time domain waveform $s(t)$. However, this would not be as complicated for the envelope as it would for the sonagram, so that taking the peak of the envelope as time of click arrival might be a good and perhaps more accurate alternative for the method that was used (although it would be more difficult to program).

Provided solutions to problems of recording clicks at sea

The use of the four hydrophone array provided solutions to three of the four problems that are normally encountered when recording clicks of free-ranging odontocetes. First of all, source levels of clicks could be determined with accuracy up to ranges of 25 m. The large error in range estimation at large ranges is partly accounted for by the $20 \log R$ term in the equation for source level, so that the error in source level estimation is only one to a few dB larger at large ranges than at small ranges. By looking at the array calibration results, rather than the theoretical error in range estimation, the error in source level estimation at $R = 25$ m did not exceed 1.5 dB, and at $R = 10$ m it didn't exceed 0.5 dB. Although it may seem justifiable to use ranges larger than 30 m for source level estimations as well, this should not be done because Fig. 2 shows that ranges (and therefore source levels) cannot be calculated with any accuracy for $R > 30$ m.

Second, discrimination between actual clicks and surface reflections was easier than it would be for the one hydrophone situation. This also made it possible to discriminate between double click recordings and surface reflections, thereby showing the existence of such double clicks unambiguously. Double pulses were also reported for Hector's dolphin (*Cephalorhynchus hectori*) by Dawson (1988), Dawson (1991), and Thorpe et al. (1991), and for Commerson's dolphin (*C. commersonii*) by Evans et al. (1988). However, as argued by Au (1993: 136), to exclude the possibility of the second click being surface reflection in the one hydrophone situation, several consecutive clicks from a moving animal should be recorded. The other way to discern second pulses from surface reflections, by looking at the mirrored amplitudes of the reflections, is much more difficult for odontocetes belonging to the second acoustic category mentioned in the Introduction (like Hector's and Commerson's dolphin) than for species of the first acoustic category. Odontocete species belonging to the second category emit echolocation pulses of much longer duration and with much more oscillations, so that any surface reflections from these pulses would resemble the actual pulses very much. Therefore, using a hydrophone array would especially be helpful for click recordings from those species.

One might suspect that the double click recordings were actually part of a whole series of quickly transmitted clicks, like a series of burst pulse clicks, that were not recorded within the 800 μ s window. However, this would have resulted in several consecutive double click recordings with interclick intervals of only 1 or 2 ms, which was not the case. Therefore, the recorded double clicks seem to be real, and their function in echolocation should be investigated in future research.

A solution was also provided to the third problem of recording clicks at sea: within certain limits of confidence, clicks could be assigned to individual animals. Some inaccuracy in assigning clicks to individuals, however, might have been caused by linking similar groups of clicks that were separated in time by one or more other groups. Linking groups of clicks that were being emitted by different animals, or not linking groups emitted by a single animal, would result in either underestimating or overestimating, respectively, the actual number of animals emitting clicks. Because of the conservative approach that was chosen in assigning clicks to individuals, it seems more

likely that the number of dolphins would have been overestimated rather than underestimated.

Despite any inaccuracy, the discriminant analyses showed that the assignments of clicks that were made resulted in highly significant differences in all click characteristics, among presumed individuals. However, in case the number of individual dolphins has indeed been overestimated, it could also mean that different click trains emitted by one dolphin were significantly different from one another, or even that different parts of a single click train were different (each of which could have been considered as one individual dolphin). Therefore, it is not clear yet whether or not each individual dolphin emitted its own type of clicks, or that each specific click train had unique click characteristics. In order to make the technique of assigning clicks to individual dolphins more powerful, it should be used in combination with good video recordings of the dolphins.

Concerning the fourth problem with click recordings from wild dolphins, the lack of video data also made it difficult to discriminate between clicks recorded from the beam axis and clicks that were off-axis. However, even without the video data, recording with a four hydrophone star array makes this discrimination easier than recording with only one hydrophone. Each click can be analyzed from the channel with the highest amplitude, in contrast to the one hydrophone situation where from the total data set only the high amplitude clicks can be analyzed. Furthermore, by subselecting all clicks of which the highest SPL was recorded by H_0 , the probability of analyzing only on-axis clicks increases even more. However, this subselection of H_0 -clicks were found not to be different in most of their mean click characteristics from the total data set, nor did their further analyses (discriminant analyses and plotting click parameters against each other) give much different results than analyzing all clicks. This might be an indication that not only H_0 -clicks, but most recorded clicks were on-axis.

Another indication that most clicks were likely to be recorded from dolphins echolocating on the array comes from the linear relationship that was found, for both the spinner dolphin and spotted dolphin clicks, between interclick interval and range, of which the linear regression equations had slopes similar to the slope of the equation for the two-way transit time of the click. However, although most clicks might have been recorded from the beam axis, some precaution should be taken when interpreting the variation in peak-to-peak source level and other click characteristics from a single click train, like the analyzed click train of the individual spotted dolphin. This recorded variation could also be a result of scanning movements of the dolphin, so that only for some clicks the center of the beam was directed at the array. Also, the several relationships that were found between click parameters could have been partially caused by scanning movements (in which case different points in the scatter plots would represent different points within the same echolocation beam). This seems not very likely, however, since the plots of center frequency on source level were very similar to the same relationship found by Au et al. (1995) for a false killer whale that was positioned at a bite plate (and thus not able to make scanning movements while performing the echolocation task).

Characteristics of the recorded clicks

The highest peak-to-peak source levels that were recorded from both spinner and spotted dolphins exceed the source level of 218 dB re 1 μ Pa recorded for narwhal (*Monodon monoceros*) clicks, at the time “the most intense sound recorded so far from an animal in nature” by Møhl et al. (1990). Furthermore, mean source levels for both spinner dolphins and spotted dolphins are much higher than maximum source levels recorded earlier for clicks of free-ranging odontocetes (175.3 dB re 1 μ Pa for *Physeter catodon* by Levenson 1974; 160 dB re 1 μ Pa for a variety of species from the geni *Delphinus*, *Lagenorhynchus*, *Stenella*, and *Tursiops* by Watkins 1980b; 150.7 dB re 1 μ Pa for *Cephalorhynchus hectori* by Dawson 1988), which brings this study in accordance with the study by Møhl and co-workers in closing the “dB gap” between wild and trained, captive odontocetes. To obtain reliable source levels for echolocation clicks of other species in the wild as well, more studies using hydrophone arrays would be desirable.

Besides high source levels, clicks from spinner dolphins and spotted dolphins are characterized by very broad bandwidths (both rms and 3-dB bandwidths), a sharp rise time with two main excursions and some minor excursions in the time domain, very short signal durations, high center frequencies (with higher SL clicks having higher center frequencies, higher 3-dB bandwidths, and better intrinsic range resolution), and both unimodal and bimodal frequency spectra with the latter type prevailing. Furthermore, these clicks are even more Doppler resistant than clicks from other odontocetes, and have the best intrinsic resolution values, to my knowledge, reported for any odontocete species so far. Spinner dolphins are known to only feed on prey items of less than 20 cm long (Norris et al. 1994). It would be interesting to look for a correlation across species between average prey size and intrinsic resolution characteristics of the clicks.

The click characteristics of both species are very much alike (although the recorded spotted dolphin clicks showed more variation than the spinner dolphin clicks) and clearly place the spinner dolphin and spotted dolphin into the first acoustic category of odontocetes, mentioned in the Introduction, that produces both short, broadband pulsed sounds as well as frequency modulated tonal sounds known as whistles. It also strengthens the validity of the hypothesized acoustic subdivision into two categories, which is increasingly supported as more species are added. Concluding, although the data set of this study was limited, and therefore no attempts have been made to associate click characteristics with behavioral mode, the characterization of spinner dolphin clicks and spotted dolphin clicks is a first step towards a better understanding of the use of echolocation in the wild by these two species.

Recommendations for further research

None of the click characteristics did show any correlation with range. However, this was not investigated for presumed individual dolphins, because no dolphin clicks were recorded of which the calculated positions showed a one-way direction of movement. To investigate whether or not dolphins use spectral adaptation of the clicks for decreasing ranges, a situation would be needed where an individual dolphin would approach the array from about 10 to a few m while echolocating on it. Good video

recordings would be needed for this, as well as to obtain certainty about the dolphin having its echolocation beam directed at the array.

Furthermore, the discrimination analysis that was applied to look for differences in click characteristics among presumed individual dolphins could also be used to look for differences in click characteristics among several behavioral modes. For example, it would be interesting to investigate whether intrinsic range resolution of the clicks has better values for foraging mode (where echolocation is used to scan for prey items) than for travelling mode (where echolocation is likely to be used for navigation). However, if individual dolphins would indeed transmit clicks with individual click characteristics, such a study could only be done with a population of known individual dolphins, like the populations studied by Herzing (1996). Long term studies of known individuals would also be necessary for answering the question if individual dolphins do indeed have unique click characteristics, or that each transmitted click train is different.

Finally, the method of localizing dolphins by recording clicks with a four hydrophone array could also be used in studies of the frequency modulated sounds, which are produced by odontocete species of the first acoustic category. Spinner dolphins seem to be able to produce clicks and whistles simultaneously (Lammers pers. comm.). Localizing whistling dolphins by use of their simultaneously produced clicks may further clarify the use of individual dolphin whistles, which are known as signature-whistles (Caldwell & Caldwell 1965; Caldwell et al. 1990). General studies that investigate the population biology of odontocetes might also be facilitated by using the array in order to track dolphins. By adjusting the data acquisition program, it should be possible to immediately and automatically display the x-y coordinates of echolocating dolphins (and either a number or color indicating depth) as pixels on a computer screen. However, for clicks that have more than one major peak in the time domain (like the clicks produced by species of the second acoustic category), it would be difficult to let the program automatically determine times of click arrival at each channel.

ACKNOWLEDGMENTS

I am very grateful to Whitlow Au for supervising me in a more than excellent way and for his proficiency and great sense of humor. I am also very grateful to Marc Lammers for assisting in the data collection, for sharing his insights in the spinner dolphin population at the Waianae coast of Oahu and for constructive comments on this report. Furthermore, I would like to thank Roland Aubauer and Dave Lemonds for useful discussions, Jennipher Philips for support in programming in Qbasic, Paul Nachtigall, Linda Choy and Claudia Aubauer for general support, and Louis Herman and Adam Pack from the Kewalo Basin Marine Mammal Laboratory for providing computer hardware and software on which part of the data analysis was carried out. I am also very grateful for the financial support provided by the Royal Dutch Academy of Sciences (KNAW), the Schuurman-Schimmel van Outeren foundation, and the faculty of Mathematics and Natural Sciences of the University of Groningen.

REFERENCES

- Au, W.W.L. (1980). Echolocation signals of the Atlantic bottlenose dolphin (*Tursiops truncatus*) in open waters. In: R.G. Busnel & J.F. Fish, eds., *Animal Sonar Systems*. Plenum Press, New York, pp. 251-282.
- Au, W.W.L. (1993). *The Sonar of Dolphins*. Springer-Verlag, New York.
- Au, W.W.L., Pawloski, J.L., Nachtigall, P.E., Blonz, M. & Gisner, R.C. (1995). Echolocation signals and transmission beam pattern of a false killer whale (*Pseudorca crassidens*). *J. Acoust. Soc. Am.* 98: 51-59.
- Aubauer, R. (1995). Korrelationsverfahren zur Flugbahnverfolgung echoortender Fledermäuse. *Fortschr.-Ber. VDI Reihe 17 Nr. 132* Düsseldorf: VDI-Verlag.
- Barrett-Lennard, L.G., Ford, J.K.B. & Heise, K.A. (1996). The mixed blessing of echolocation: differences in sonar use by fish-eating and mammal-eating killer whales. *Anim. Behav.* 51: 553-565.
- Caldwell, M.C. & Caldwell, D.K. (1965). Individualized whistle contours in bottlenosed dolphins (*Tursiops truncatus*). *Nature* 207: 434-435.
- Caldwell, M.C., Caldwell, D.K. & Tyack, P.L. (1990). Review of the signature-whistle hypothesis for the Atlantic bottlenose dolphin. In: S. Leatherwood & R.R. Reeves, eds., *The Bottlenose Dolphin*. Academic Press, San Diego, CA, pp. 199-233.
- Carder, D., Ridgway, S., Whitaker, B. & Geraci, J. (1995). Hearing and echolocation in a pygmy sperm whale *Kogia*. *Proc. 11th Biennial Conf. on the Biol. of Marine Mamm.*, Orlando, Fl., Dec. 14-18, 1995.
- Dawson, S.M. (1988). The high frequency sounds of free-ranging Hector's dolphins, *Cephalorhynchus hectori*. *Rep. Int. Whal. Commn. (Spec. Iss. 9)*: 339-344.
- Dawson, S.M. (1991). Clicks and communication: the behavioural and social contexts of Hector's dolphin vocalizations. *Ethology* 88: 265-276.
- Evans, W.E. & Awbrey, F.T. (1988). Natural history aspects of marine mammal echolocation: feeding strategies and habitat. In: P.E. Nachtigall & P.W.B. Moore, eds., *Animal Sonar: Processes and Performance*. Plenum Press, New York, pp. 521-534.
- Evans, W.E., Awbrey, F.T. & Hackbarth, H. (1988). High frequency pulses produced by free-ranging Commerson's dolphin (*Cephalorhynchus commersonii*) compared to those of Phocoenids. *Rep. Int. Whal. Commn. (Spec. Iss. 9)*: 173-181.
- Fenton, M.B. (1980). Adaptiveness and ecology of echolocation in terrestrial (aerial) systems. In: R.G. Busnel & J.F. Fish, eds., *Animal Sonar Systems*. Plenum Press, New York, pp. 427-446.
- Gabor, D. (1947). Acoustical quanta and the theory of hearing. *Nature* 159: 591-595.
- Herzing, D.L. (1996). Vocalizations and associated underwater behavior of free-ranging Atlantic spotted dolphins, *Stenella frontalis* and bottlenose dolphins, *Tursiops truncatus*. *Aq. Mammals* 22(2): 61-79.
- Kammaing, C., van Hove, M.T., Engelsma, F.J. & Terry, R.P. (1993). Investigations on cetacean sonar X: a comparative analysis of underwater echolocation clicks of *Inia* spp. and *Sotalia* spp. *Aq. Mammals* 19(4): 31-43.
- Levenson, C. (1974). Source level and bistatic target strength of the sperm whale (*Physeter catodon*) measured from an oceanographic aircraft. *J. Acoust. Soc. Am.* 55: 1100-1103.
- Lindeman, R.H., Merenda, P.F. & Gold, R.Z. (1980). *Introduction to Bivariate and Multivariate Analysis*. Scott, Foresman and Company, Glenview, IL.

- Magyar, I., Schleidt, W.M. & Miller, B. (1978). Localization of sound producing animals using the arrival time differences of their signals at an array of microphones. *Experientia* 34(5): 676-677.
- McBride, A.F. (1956). Evidence for echolocation by cetaceans. *Deep-Sea Research* 3: 153-154.
- Møhl, B., Surlykke, A. & Miller, L.A. (1990). High intensity narwhal clicks. In: J. Thomas & R. Kastelein, eds., *Sensory Abilities of Cetaceans*. Plenum Press, New York, pp. 295-303.
- Norris, K.S. & Møhl, B. (1983). Can odontocetes debilitate prey with sound? *Am. Natur.* 122(1), 85-104.
- Norris, K.S., Wursig, B., Wells, R.S. & Wursig, M. (1994). *The Hawaiian Spinner Dolphin*. University of California Press, Berkeley, CA.
- Thomas, J.A., Fisher, S.R. & Ferm, L.M. (1986). Acoustic detection of cetaceans using a towed array of hydrophones. *Rep. Int. Whal. Commn. (Spec. Iss. 8)*: 139-148.
- Thorpe, C.W., Bates, R.H.T. & Dawson, S.M. (1991). Intrinsic echolocation capability of Hector's dolphin, *Cephalorhynchus hectori*. *J. Acoust. Soc. Am.* 90: 2931-2934.
- Watkins, W.A. (1980a). Acoustics and the behavior of sperm whales. In: R.G. Busnel & J.F. Fish, eds., *Animal Sonar Systems*. Plenum Press, New York, pp. 283-290.
- Watkins, W.A. (1980b). Click sounds from animals at sea. In: R.G. Busnel & J.F. Fish, eds., *Animal Sonar Systems*. Plenum Press, New York, pp. 291-297.
- Watkins, W.A. & Schevill, W.E. (1974). Listening to Hawaiian spinner porpoises, *Stenella cf. longirostris*, with a three-dimensional hydrophone array. *J. Mammal.* 55: 319-328.
- Wood, F.G. & Evans, W.E. (1980). Adaptiveness and ecology of echolocation in toothed whales. In: R.G. Busnel & J.F. Fish, eds., *Animal Sonar Systems*. Plenum Press, New York, pp. 381-425.
- Zar, J.H. (1984). *Biostatistical Analysis*. Prentice-Hall, Englewood Cliffs, NJ.

APPENDIX

Direct and surface reflected paths to the four hydrophones

The angle between two vectors \underline{a} and \underline{b} , $\angle(\underline{a}, \underline{b})$, can be written as:

$$\cos\angle(\underline{a}, \underline{b}) = \frac{\underline{a} \cdot \underline{b}}{|\underline{a}| \cdot |\underline{b}|}$$

where $\underline{a} \cdot \underline{b} = a_x \cdot b_x + a_y \cdot b_y + a_z \cdot b_z$,

and where $|\underline{a}|$ and $|\underline{b}|$ are the absolute sizes of these vectors.

Range R can also be written as a vector, by subtracting the x , y , z coordinates of the echolocating dolphin ($R \cdot \cos\phi \cdot \cos\theta$, $R \cdot \sin\phi \cdot \cos\theta$, $R \cdot \sin\theta$) from the coordinates of H_0 ($0, 0, 0$). Therefore:

$$\underline{R} = (R \cdot \cos\phi \cdot \cos\theta, R \cdot \sin\phi \cdot \cos\theta, R \cdot \sin\theta)$$

Furthermore, three vectors (\underline{a}_1 , \underline{a}_2 , and \underline{a}_3) can be described from H_0 to each of the outer hydrophones H_1 , H_2 , and H_3 , being the coordinates of H_1 , H_2 , and H_3 . Since the angle between \underline{a}_1 and the y -axis is 30° (see Fig. 1 on page 5), the y and z coordinates of H_1 are $-(\sqrt{3}/2) \cdot a$ and $0.5 \cdot a$, respectively. H_2 has y and z coordinates of $(\sqrt{3}/2) \cdot a$ and $0.5 \cdot a$. Therefore:

$$\underline{a}_1 = (0, -(\sqrt{3}/2) \cdot a, 0.5 \cdot a)$$

$$\underline{a}_2 = (0, (\sqrt{3}/2) \cdot a, 0.5 \cdot a)$$

$$\underline{a}_3 = (0, 0, -a)$$

Now, three angles (α_1 , α_2 , and α_3) can be defined between \underline{R} and each of \underline{a}_1 , \underline{a}_2 , and \underline{a}_3 :

$$\alpha_1 = \angle(\underline{a}_1, \underline{R})$$

$$\alpha_2 = \angle(\underline{a}_2, \underline{R})$$

$$\alpha_3 = \angle(\underline{a}_3, \underline{R})$$

Now:

$$\cos(\alpha_1) = \frac{a_1 \cdot R}{|a_1| \cdot |R|} = -(\sqrt{3}/2) \cdot \sin\varphi \cdot \cos\theta + 0.5 \cdot \sin\theta$$

$$\cos(\alpha_2) = \frac{a_2 \cdot R}{|a_2| \cdot |R|} = (\sqrt{3}/2) \cdot \sin\varphi \cdot \cos\theta + 0.5 \cdot \sin\theta$$

$$\cos(\alpha_3) = \frac{a_3 \cdot R}{|a_3| \cdot |R|} = -\sin\theta$$

Furthermore, by looking at Fig. A1, the absolute size of R_3 (which is R_3) can be expressed by using the cosine rule:

$$\begin{aligned} R_3 &= \sqrt{R^2 + a^2 - 2 \cdot a \cdot R \cdot \cos(\alpha_3)} \\ &= \sqrt{R^2 + a^2 + 2 \cdot a \cdot R \cdot \sin\theta} \end{aligned}$$

In the same way, R_1 and R_2 can be derived:

$$\begin{aligned} R_1 &= \sqrt{R^2 + a^2 - 2 \cdot a \cdot R \cdot \cos(\alpha_1)} \\ &= \sqrt{R^2 + a^2 + a \cdot R \cdot \sqrt{3} \cdot \sin\varphi \cdot \cos\theta - a \cdot R \cdot \sin\theta} \end{aligned}$$

$$\begin{aligned} R_2 &= \sqrt{R^2 + a^2 - 2 \cdot a \cdot R \cdot \cos(\alpha_2)} \\ &= \sqrt{R^2 + a^2 - a \cdot R \cdot \sqrt{3} \cdot \sin\varphi \cdot \cos\theta - a \cdot R \cdot \sin\theta} \end{aligned}$$

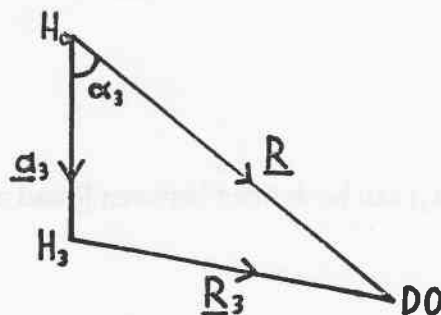


Fig. A1. The absolute size of vector R_3 can be calculated if α_3 is known, using the cosine rule. DO is the position of the dolphin.

The vectors \underline{R}_1 , \underline{R}_2 , and \underline{R}_3 can be obtained by subtracting the coordinates of H_1 , H_2 , and H_3 , respectively, from the coordinates of the dolphin (which is the same as subtracting \underline{a}_1 , \underline{a}_2 , and \underline{a}_3 , respectively, from \underline{R}):

$$\underline{R}_1 = (R \cdot \cos\phi \cdot \cos\theta, R \cdot \sin\phi \cdot \cos\theta + (\sqrt{3}/2) \cdot a, R \cdot \sin\theta - 0.5 \cdot a)$$

$$\underline{R}_2 = (R \cdot \cos\phi \cdot \cos\theta, R \cdot \sin\phi \cdot \cos\theta - (\sqrt{3}/2) \cdot a, R \cdot \sin\theta - 0.5 \cdot a)$$

$$\underline{R}_3 = (R \cdot \cos\phi \cdot \cos\theta, R \cdot \sin\phi \cdot \cos\theta, R \cdot \sin\theta + a)$$

Fig. A2 shows that the length of the surface reflected path SR_3 from the dolphin to the deepest hydrophone H_3 is equal to the length of the path from the dolphin to a imaginary hydrophone H_3' , positioned on the z-axis at a same distance above the water surface as the depth of H_3 (which is depth D of $H_0 + a$). Now, the vector \underline{X}_3 is defined as the vector from H_3 to H_3' :

$$\underline{X}_3 = (0, 0, 2 \cdot D + 2 \cdot a)$$

Also, since the depths of H_1 and H_2 are $D - 0.5 \cdot a$, the vectors \underline{X}_0 , \underline{X}_1 , and \underline{X}_2 can be expressed as:

$$\underline{X}_0 = (0, 0, 2 \cdot D)$$

$$\underline{X}_1 = \underline{X}_2 = (0, 0, 2 \cdot D - a)$$

Now, the four angles β_0 , β_1 , β_2 , and β_3 can be defined as:

$$\beta_0 = \angle(\underline{X}_0, \underline{R})$$

$$\beta_1 = \angle(\underline{X}_1, \underline{R}_1)$$

$$\beta_2 = \angle(\underline{X}_2, \underline{R}_2)$$

$$\beta_3 = \angle(\underline{X}_3, \underline{R}_3)$$

And:

$$\cos(\beta_0) = \frac{X_0 \cdot R}{|X_0| \cdot |R|} = \sin\theta$$

$$\cos(\beta_1) = \frac{X_1 \cdot R_1}{|X_1| \cdot |R_1|} = (R \cdot \sin\theta - 0.5 \cdot a) / R_1$$

$$\cos(\beta_2) = \frac{X_2 \cdot R_2}{|X_2| \cdot |R_2|} = (R \cdot \sin\theta - 0.5 \cdot a) / R_2$$

$$\cos(\beta_3) = \frac{X_3 \cdot R_3}{|X_3| \cdot |R_3|} = (R \cdot \sin\theta + a) / R_3$$

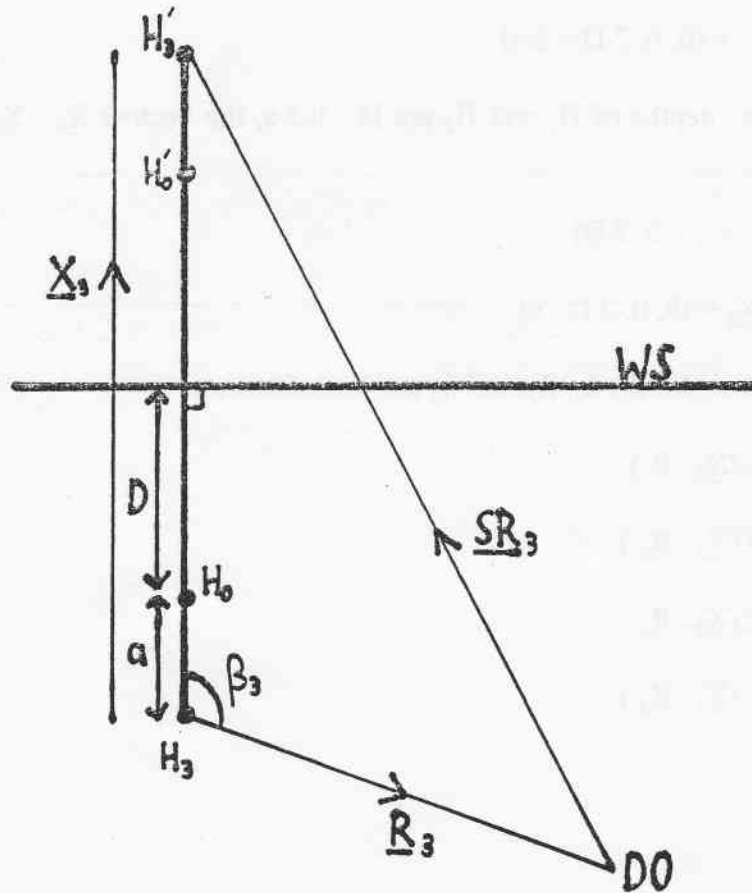


Fig. A2. The surface reflected path SR_3 to the third hydrophone can be calculated if β_3 is known, using the cosine rule. DO is the position of the dolphin, WS is the water surface.

Now, SR_3 can be derived from Fig. A2 by using the cosine rule:

$$SR_3 = \sqrt{R_3^2 + (2 \cdot D + 2 \cdot a)^2 - 2 \cdot R_3 \cdot (2 \cdot D + 2 \cdot a) \cdot \cos(\beta_3)}$$

Similarly:

$$SR_0 = \sqrt{R^2 + (2 \cdot D)^2 - 2 \cdot R \cdot (2 \cdot D) \cdot \cos(\beta_0)}$$

$$SR_1 = \sqrt{R_1^2 + (2 \cdot D - a)^2 - 2 \cdot R_1 \cdot (2 \cdot D - a) \cdot \cos(\beta_1)}$$

$$SR_2 = \sqrt{R_2^2 + (2 \cdot D - a)^2 - 2 \cdot R_2 \cdot (2 \cdot D - a) \cdot \cos(\beta_2)}$$

By substituting for $\cos(\beta_i)$ and for R_i , we obtain:

$$SR_0 = \sqrt{R^2 + 4 \cdot D^2 - 4 \cdot R \cdot D \cdot \sin\theta}$$

$$SR_1 = \sqrt{R^2 + 4 \cdot D^2 - 3 \cdot a \cdot D + 1.5 \cdot a^2 + a \cdot R \cdot \sqrt{3} \cdot \sin\varphi \cdot \cos\theta - 2 \cdot R \cdot D \cdot \sin\theta}$$

$$SR_2 = \sqrt{R^2 + 4 \cdot D^2 - 3 \cdot a \cdot D + 1.5 \cdot a^2 - a \cdot R \cdot \sqrt{3} \cdot \sin\varphi \cdot \cos\theta - 2 \cdot R \cdot D \cdot \sin\theta}$$

$$SR_3 = \sqrt{R^2 + 4 \cdot D^2 + 4 \cdot a \cdot D + a^2 - 2R \cdot (2D + a) \cdot \sin\theta}$$

Distributions of several click characteristics

